CATÓLICA
ESCOLA SUPERIOR DE BIOTECNOLOGIA
PORTO

Development of a Tunnel Filler to Address Anchoring and Fixation Challenges in Knee Ligaments Reconstruction

By:
Rui Paulo Santos Moreira

Porto, December 2024

CATÓLICA
ESCOLA SUPERIOR DE BIOTECNOLOGIA
PORTO

Development of a Tunnel Filler to Address Anchoring and Fixation Challenges in Knee Ligaments Reconstruction

Dissertation presented to Escola Superior de Biotecnologia da Universidade Católica Portuguesa do Porto to fulfil the necessary requirements to obtain the master's degree in Biomedical Engineer.

By:
Rui Paulo Santos Moreira

Under the supervision of João Pedro Bebiano Costa, Ph.D,
Under the co-supervision of Viviana Pinto Ribeiro, Ph.D

Porto, December 2024

“A Alma é divina,

E a obra é imperfeita”

- Fernando Pessoa, *Mensagem*

Acknowledgment

First, I would like to express my deepest gratitude to my supervisors, João Costa and Viviana Ribeiro, for the opportunity to work under their guidance. Your help, support, and invaluable insights have been instrumental in completing this work.

I am also sincerely thankful to Professor Ana Oliveira, for her expert guidance and for sharing her wealth of experience, which has been a source of inspiration throughout this journey.

A special thanks to Inês Vasconcelos for always being there to help with anything I needed in the lab, for the laughter and friendship we shared, and for teaching me so much along the way.

I would like to acknowledge everyone in the 142 Biomaterials lab. Thank you all for the friendship, the shared moments, the assistance, and the knowledge that made this experience unforgettable.

To my friend Mafalda, who worked alongside me in the lab on a related topic for her thesis, thank you for your invaluable help, collaboration, and teamwork. It was a true pleasure to work with you. To Eduardo and André, I deeply appreciate the time we spent together, the knowledge you shared, and your support. Your help was indispensable throughout this process.

I am also deeply grateful to all my friends. Thank you for your constant support and for simply being my friends. Your presence made this journey much easier.

A heartfelt thanks to my parents, my brother, my girlfriend and my (official) sister-in-law. You have supported me through every step of my life. You are the most important part of my journey, and without you, this achievement would not have been possible.

Finally, I thank God, for always being by my side, supporting and guiding me through every step of my journey.

Abstract

Knee ligament injuries, especially anterior cruciate ligament (ACL) injuries, are a prevalent concern in orthopedic sports medicine, often demanding surgical intervention to restore knee stability and function. Common challenges encountered during ligament reconstruction procedures include anchoring and fixation issues. Traditional methods, while effective, frequently result in complications such as tunnel widening, graft slippage, and inadequate fixation strength. This research introduces a novel tunnel filler (TF) that not only aims to overcome these limitations related to fixation stability of the graft but also promotes effective osteointegration within the fixation tunnel. The primary objectives of this project were to design, fabricate, and evaluate a TF using 3D printing technology with polycaprolactone (Pcl), and to enhance its structural support and biological activity with Pcl electrospun fibers and brushite (Brh).

A series of comprehensive tests was conducted to characterize the TF. Physicochemical analysis confirmed the stability and integrity of the material composition. Mechanical testing demonstrated the TF's enhanced durability under physiological loads. Surface roughness analysis, performed using Scanning Electron Microscopy (SEM), showed improvements in texture that could facilitate cellular adhesion. *In vitro* cell culture testing, with Alamar Blue and Live/Dead assays, indicated effective cell interaction and good biocompatibility. By the end of the study, these enhancements contributed to the development of a TF with good mechanical properties and non-toxic for the cells

Keywords: Ligaments fixation, tunnel filler, 3D printing, electrospinning, Polycaprolactone.

Resumo

As lesões nos ligamentos do joelho, especialmente lesões no ligamento cruzado anterior (LCA), são uma preocupação prevalente na medicina desportiva ortopédica, frequentemente exigindo intervenção cirúrgica para restaurar a estabilidade e função do joelho. Os desafios mais comuns encontrados durante os procedimentos de reconstrução de ligamentos incluem problemas de ancoragem e fixação. Os métodos tradicionais, embora eficazes, frequentemente resultam em complicações como alargamento do túnel ósseo, deslizamento do enxerto e força de fixação inadequada. Esta pesquisa introduz um novo "Tunnel Filler" (TF) que não só visa superar estas limitações relacionadas com a estabilidade de fixação do enxerto, mas também promover uma osteointegração eficaz dentro do túnel ósseo. Os objetivos primários deste projeto foram desenhar, fabricar e avaliar um TF utilizando a tecnologia de impressão 3D com policaprolactona (Pcl), e melhorar o seu suporte estrutural e atividade biológica com fibras eletrofiadas de Pcl e brushite (Brh).

Uma série de testes foram realizados para caracterizar o TF. A análise físico-química confirmou a estabilidade e integridade da composição do material. Os testes mecânicos demonstraram a durabilidade aprimorada do TF sob cargas fisiológicas. A análise da rugosidade superficial, realizada usando Microscopia Eletrónica de Varredura (SEM), mostrou melhorias na textura que poderiam facilitar a adesão celular. Os testes de cultura celular *in vitro*, com ensaios de Alamar Blue e Live/Dead, indicaram uma interação celular eficaz e boa biocompatibilidade. No final do estudo, estas melhororias contribuíram para o desenvolvimento de um TF com boas propriedades mecânicas e não tóxico para as células.

Palavras-chave: Fixação de ligamentos, preenchimento de túnel, impressão 3D, eletrofiação, Policaprolactona.

List of Abbreviations

3D – Three-Dimensional

ACL – Anterior Cruciate Ligament

Brh – Brushite

DCPD – Dicalcium Phosphate Dihydrate

DMEM – Dulbecco's Modified Eagle Medium

DMSO – Dimethyl Sulfoxide

FBS – Fetal Bovine Serum

FTIR – Fourier-transform infrared spectroscopy

LCL – Lateral Collateral Ligament

MCL – Medial Collateral Ligament

PBS – Phosphate-buffered saline

Pcl – Polycaprolactone

PCL – Posterior Cruciate Ligament

PI – Propidium Iodide

PLA – Polylactic Acid

PVA – Polyvinyl Alcohol

SED – Secondary Electron Detector

SEM – Scanning Electron Microscopy

TF –Tunnel Filler

TFE – Tunnel Filler with Electrospun Fibber

TFE + Brh – Tunnel Filler with Electrospunn Fibbers and Brushite

UCS – Ultimate Compressive Strength

UTS – Ultimate Tensile Strength

Contents

List of Figures

List of Tables

1. Introduction

1.1. Objectives of the project

The primary objective of this project is to develop a Tunnel Filler (TF) that addresses the prevalent fixation and anchoring failures encountered in ligament reconstruction surgeries. These failures, as discussed earlier, pose significant challenges to the success and longevity of the graft, often leading to complications such as graft slippage, tunnel widening, and eventual failure,

The development process of the TF begins with the selection and 3D printing of a suitable model. The 3D printed TF is designed to fit precisely within the bone tunnel, ensuring optimal contact with the surrounding bone tissue. After printing, the TF undergoes an electrospinning process, where it is coated with thin Pcl fibers. To finalize the production process, the TF, is coated with Brh.

To ensure the TF meets the required mechanical and chemical standards, a series of characterization tests are conducted. These tests include Scanning Electron Microscopy (SEM) to analyse the surface morphology, Fourier Transform Infrared Spectroscopy (FTIR) for chemical characterization, and swelling tests to assess the material's interaction with fluids. Mechanical properties are further assessed through tension and compression tests Additionally, cytotoxicity tests, including Alamar Blue and Live/Dead assays, are performed to evaluate the biocompatibility of the TF.

1.2. The knee: functions and composition

The knee is a complex and essential joint in the human body, serving multiple functions and composed of various structures that contribute to its stability, movement, and overall function. This tissue works as a pivot, permitting flexion and expansion developments, which are essential for exercises like strolling, running, sitting, and standing. However, it also allows for a small amount of rotation, which is crucial for the lower limb's alignment and movement. During dynamic activities like walking or jumping, the knee plays a crucial role in weight bearing and load transmission [1]. Beyond

its structural role, the knee joint is involved in neurosensory functions, providing feedback to the central nervous system about the stresses applied to the ligaments. This feedback mechanism is essential for coordinating muscle responses to maintain joint stability and prevent injury [1].

The knee joint is composed of three main bones: the femur (thigh bone), the tibia (shin bone), and the patella (kneecap) (Figure 1). These bones are connected by a complex system of ligaments, tendons, and cartilage that ensures stability and smooth movements.

- **Ligaments:** The knee contains four major ligaments:
    - Anterior Cruciate Ligament (ACL): Prevents the tibia from sliding out in front of the femur.
    - Posterior Cruciate Ligament (PCL): Prevents the tibia from sliding backward.
    - Medial Collateral Ligament (MCL): Provides stability to the inner knee.
    - Lateral Collateral Ligament (LCL): Provides stability to the outer knee [1].
- **Menisci:** The knee joint also includes two menisci, which are crescent-shaped cartilages that act as shock absorbers between the femur and tibia. They help distribute the body's weight across the knee joint, reducing the stress on the bones and cartilage [1].
- **Cartilage:** The articular cartilage covers the ends of the femur, tibia, and the back of the patella, providing a smooth, lubricated surface for movement and reducing friction [2].
- **Tendons and Muscles:** The quadriceps and hamstring muscles are connected to the bones via tendons, such as the patellar tendon, which is crucial for knee extension [1].

The knee's ability to perform its functions relies on the intricate coordination of these components. Injuries or degenerative changes in any of these structures can significantly impair knee function and mobility [1;2].

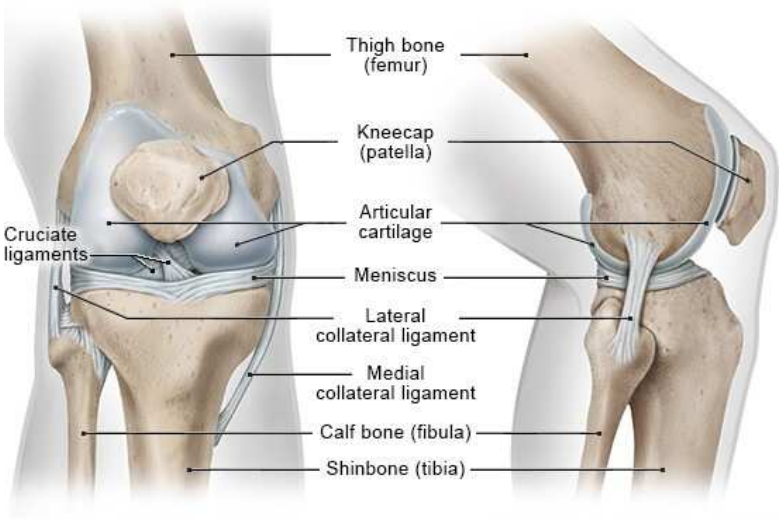

Figure 1 *- Constituents of the knee. Adapted from [1]*

1.3. Knee ligament injuries

Knee ligament injuries are among the most common and debilitating injuries, particularly for athletes and those engaged in physically demanding activities. These injuries often involve damage to one or more of the four primary ligaments in the knee: the ACL, PCL, MCL, LCL. The most frequent types of knee ligament injuries include sprains, partial tears, and complete ruptures. Among these, ACL injuries are the most prevalent, especially in sports that require sudden changes in direction, jumping, or quick deceleration, such as basketball, soccer, and skiing [2;1]. ACL injuries often occur due to non-contact mechanisms, where the knee twists or pivots while the foot remains planted on the ground. This can result in a complete tear, leading to significant instability in the knee [2]. MCL injuries are also common and usually result from a direct blow to the outside of the knee, causing it to bend inward. These injuries often occur in contact sports like football or hockey [2]. PCL injuries, though less common, typically result from a direct impact to the front of the knee, such as in a car accident or a fall onto a bent knee. LCL injuries are the least common and are often caused by a blow to the inside of the knee, pushing it outward [2].

Several factors influence the prevalence of knee ligament injuries, including biomechanical, anatomical, and environmental factors (Figure 2). Biomechanical factors such as poor movement mechanics, muscle imbalances, and insufficient neuromuscular control can increase the risk of ligament injuries [1;3]. Anatomical factors, such as the

alignment of the lower limb and the width of the intercondylar notch (where the ACL passes through the femur), can also predispose individuals to certain injuries [3]. Gender is another significant factor influencing injury prevalence. Studies have shown that female athletes are more likely to suffer from ACL injuries compared to their male counterparts. This disparity is thought to be due to a combination of hormonal differences, anatomical variations, and differences in neuromuscular control [2]. Environmental factors, such as the type of playing surface, footwear, and weather conditions, can also contribute to the likelihood of sustaining a knee ligament injury [3].

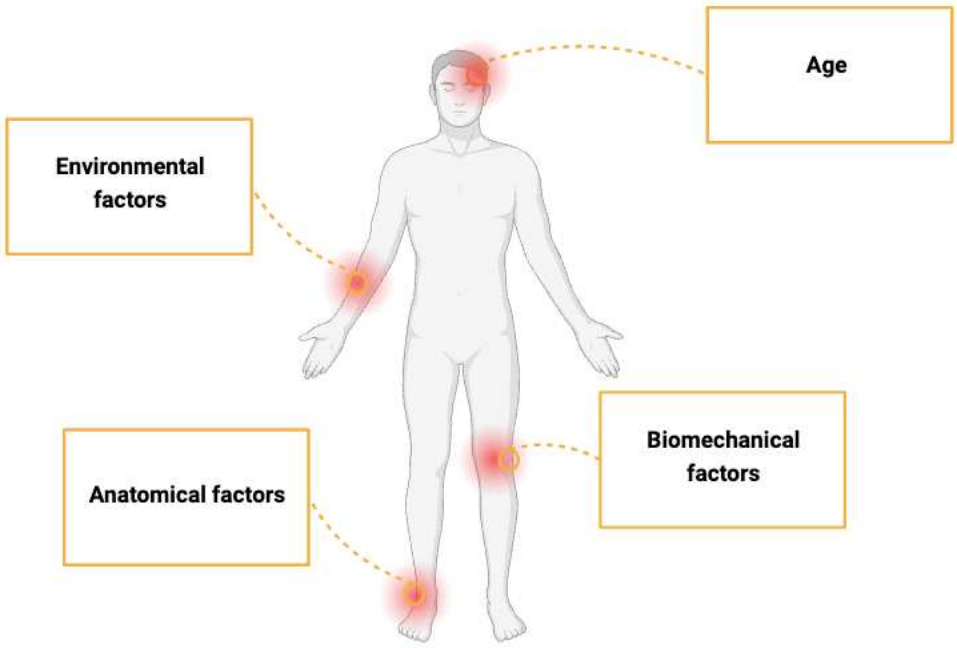

Figure 2 *- Factors influencing the prevalence of injuries in the knee*

Among all knee ligament injuries, ACL injuries are particularly significant due to their frequency and the severe impact they can have on an individual's athletic career and quality of life (Figure 3). The ACL is crucial for maintaining the stability of the knee joint, particularly during dynamic movements. An injury to the ACL often results in the need for surgical intervention and a long rehabilitation period, which can last from six months to a year or more [1;4]. The rehabilitation process for ACL injuries is extensive, involving both physical therapies to restore range of motion and strength, and neuromuscular training to prevent re-injury. Despite advances in surgical techniques and

rehabilitation protocols, not all individuals return to their pre-injury level of performance, highlighting the importance of prevention strategies in at-risk populations [2].

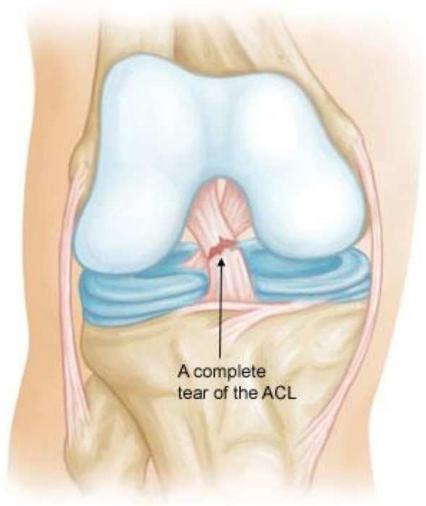

Figure 3 *- ACL complete rupture. Adapted from [5]*

1.4. Current available treatments for knee injuries

Knee injuries, particularly those involving the ACL, are a significant concern in both athletic and general populations affecting approximately 1 in 3500 people each year globally [6]. The treatment landscape for these injuries has evolved considerably, offering a range of options that vary in their mechanisms, effectiveness, and potential drawbacks [7]. This analysis explores the available treatments, their positive aspects, and the inefficiencies that persist, particularly emphasizing the challenges related to graft fixation and anchoring.

There are different approaches to treat knee injuries:

- **Surgical Interventions**: ACL reconstruction is the gold standard for treating severe knee injuries. The surgery involves replacing the torn ligament with a graft, either an autograft (from the patient's own body) or an allograft (donor tissue). The surgical process includes drilling tunnels into the femur and tibia to anchor the graft, which then serves as a new ligament. The correct positioning and fixation of the graft are crucial for the success of the surgery, as they directly affect the knee's stability and function. Post-operative management is also vital,

including controlled physical activity, pain management, and monitoring for complications such as infection, graft failure, or arthrofibrosis to ensure the graft's integration and the overall success of the surgery [10;4;7].

- **Non-Surgical Interventions:** For less severe injuries or when surgery is not an option, non-surgical treatments are utilized. These include bracing, activity modification, and targeted physical therapy aimed at managing symptoms and improving knee function without invasive procedures. Physical therapy is particularly important, both as a standalone approach and post-surgery, focusing on restoring strength, flexibility, and stability in the knee joint through exercises, manual therapy, and modalities like ultrasound. These non-surgical interventions not only aid in recovery but also help prevent future injuries by enhancing neuromuscular control [8;9]

The advancements in ACL reconstruction techniques have led to high success rates, particularly when the graft is properly positioned and secured. Studies have shown that patients often regain significant knee function and return to their previous levels of activity following successful reconstruction [10]. For instance, the use of autografts, such as the semitendinosus tendon, has been associated with lower morbidity and faster recovery compared to patellar tendon grafts [7]. Physical therapy, both as a primary treatment and as part of post-surgical rehabilitation, offers substantial benefits. It enhances muscle strength, improves joint stability, and accelerates the return to normal activities. Moreover, non-surgical interventions provide a valuable alternative for patients who cannot undergo surgery, helping to maintain knee function and quality of life [8;9].

Despite the advances in knee injury treatments, some inefficiencies remain, particularly in graft fixation and anchoring during ACL reconstruction (Table 1). A significant challenge is ensuring the anatomical placement of the graft. Studies have shown that improper tunnel placement can lead to non-anatomical graft orientation, which compromises knee stability and increases the risk of graft failure [10]. Hosseini *et al.* (2012) [10] found that both tibial and femoral tunnel misplacements are common causes of failed ACL reconstructions, leading to a graft orientation that does not replicate the

natural biomechanics of the knee. Additionally, the method of graft fixation plays a critical role in the success of ACL reconstruction. Inadequate fixation can result in graft laxity or failure. Woo *et al.* (2006) [4] highlighted that traditional fixation techniques might not provide sufficient stability, particularly in high-demand patients, leading to increased rates of re-injury. The lack of robust anchoring can also affect the integration of the graft, especially with allografts, which may not incorporate as effectively as autografts [8].

The choice between autografts and allografts also contributes to surgical ineffectiveness. While autografts generally integrate well, allografts carry a risk of disease transmission and often exhibit slower integration, leading to weaker long-term outcomes. This issue is compounded by the fact that allografts may be more prone to stretching over time, which can compromise knee stability [9]. Moreover, post-operative complications, such as arthrofibrosis (excessive scar tissue leading to joint stiffness), infection, and graft failure, remain significant concerns. Effective management of these complications is crucial, yet it is often challenging, particularly when dealing with complex or revision cases. The inefficiency in addressing these complications can lead to prolonged recovery times and suboptimal outcomes [10; 4].

Table 1 *- Inefficiency of the knee injuries treatments*

Factor	**Influence on ACL Reconstruction Prevalence**
Anatomical Placement of the graft	Incorrect tunnel placement (tibial and femoral) can lead to non-anatomical graft orientation, compromising knee stability and increasing graft failure risk [10]
Graft fixation method	Inadequate fixation can result in graft laxity or failure. Traditional techniques may not provide sufficient stability, particularly in high-demand patients, increasing re-injury rates [4]
Graft material choice	Autografts generally integrate well, but allografts carry a risk of disease transmission, exhibit slower integration, and are more prone to stretching, leading to weaker long-term outcomes [8;9]

Post-operative complications	Complications such as arthrofibrosis, infection, and graft failure are significant concerns. Inefficient management of these can prolong recovery and result in suboptimal outcomes [7;4]

1.5. Current available graft fixation methods

Graft fixation is crucial in ACL reconstruction surgery, and the success of the procedure heavily relies on the chosen fixation method [12]. Various fixation devices and techniques have been developed over the years, each with distinct advantages and drawbacks [11;13]. This section examines the main graft fixation methods currently in use, discussing their strengths and weaknesses, and highlighting the prevalent issues related to fixation and anchoring failures.

Interference Screws

Interference screws are among the most used devices for ACL graft fixation, especially in securing the graft within the tibial and femoral tunnels (Figure 4). These screws compress the graft against the tunnel walls, providing strong initial fixation that facilitates graft integration. Bioabsorbable screws, such as the BioScrew®, are particularly beneficial because they eliminate the need for hardware removal and reduce the risk of imaging artifacts during postoperative assessments [11]. However, the use of interference screws also comes with significant challenges. One of the primary issues is the potential for graft damage during insertion, particularly when metal screws are used [12]. This can lead to complications such as graft fraying or tearing, which can undermine the stability of the reconstruction. Furthermore, improper screw placement can cause tunnel widening over time, leading to graft laxity and an increased risk of failure. The reliance on bone quality also means that patients with poor bone density may experience less effective fixation [12;11].

Figure 4 *- Interference screws application. Adapted from [13]*

Suspensory Fixation Devices

Suspensory fixation devices can be categorized into fixed-loop and adjustable-loop types, both widely used for femoral fixation (Figure 5).

- **Fixed-Loop Devices**: Fixed-loop devices, such as the EndoButton™, provide reliable fixation with minimal risk of slippage. These devices are straightforward to use and offer consistent tension, making them a popular choice in ACL reconstruction [14]. However, the inability to adjust the tension post-fixation can be a significant limitation. If the initial tensioning is not optimal, the graft may become lax over time, compromising the stability of the reconstruction. Moreover, over-drilling to accommodate the device can shorten the effective tunnel length, potentially hindering graft incorporation [11].
- **Adjustable-Loop Devices**: Adjustable-loop devices, such as the TightRope®, offer the advantage of tensioning the graft after it has been fixed, providing greater control over the final tension. This can lead to improved initial stability and reduce the risk of graft laxity [14]. However, concerns have been raised about the durability of these devices. The "bungee cord effect," where the loop elongates under repeated loading, has been observed in some cases, leading to gradual loosening of the graft. This effect can reduce the overall effectiveness of the reconstruction and increase the risk of graft failure [11].

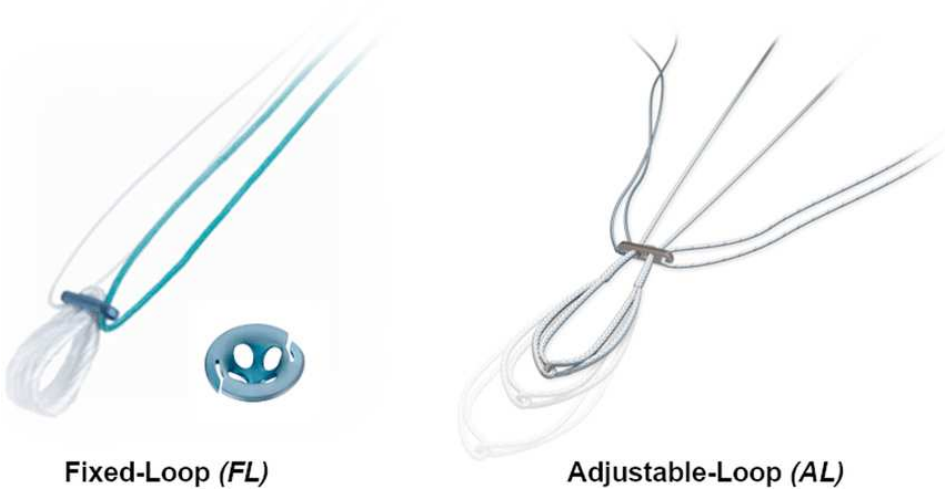

Figure 5 *- Fixed and Adjustable Loop. Adapted from [15]*

Cross-Pin Systems

Cross-pin systems provide robust fixation by securing the graft perpendicular to the bone tunnel (Figure 6). This method offers excellent initial stability and is particularly effective in preventing rotational instability, which is a common issue in ACL injuries [12]. However, the complexity of the insertion technique is a significant drawback. Precise placement is required for cross-pins, increasing the risk of tunnel misalignment, which can compromise the fixation strength. Hardware-related complications, such as pin migration or breakage, may also occur, necessitating further surgical intervention [11].

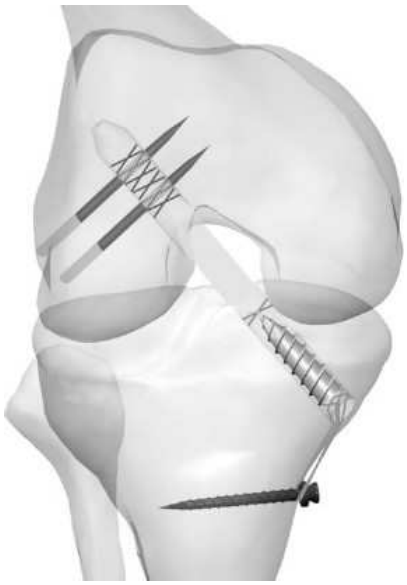

Figure 6 *- Cross-pin surgical system. Adapted from [16]*

Intra tunnel Fixation

Intra tunnel fixation methods, such as using screw and washer or bioabsorbable devices, compress the graft directly within the tunnel, enhancing the bone-graft interface and promoting biological integration (Figure 7). This method minimizes the risk of tunnel widening and reduces complications associated with external hardware [12]. However, achieving consistent tension across the graft can be challenging, particularly when dealing with variable graft diameters. The effectiveness of this method is also highly dependent on bone quality, making it less reliable in patients with osteoporosis or other bone density issues [11].

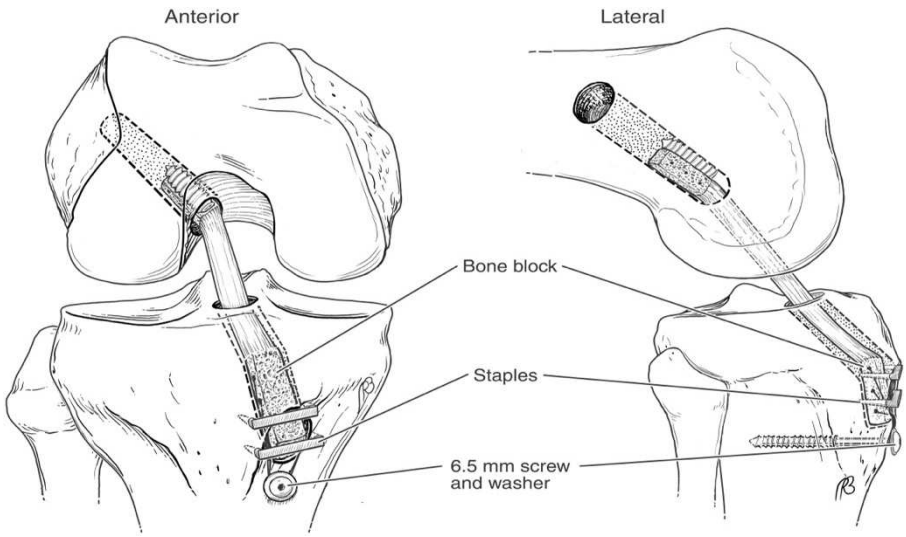

Figure 7*- Screw and washer implementation with an anterior and lateral view. Adapted from [17]*

Hybrid Fixation Techniques

Hybrid fixation techniques combine elements of different fixation methods to optimize graft stability (Figure 8). For example, combining a suspensory device with an interference screw can provide both immediate stability and long-term graft incorporation. These techniques are particularly useful in complex cases where a single fixation method may be insufficient [14]. However, the increased complexity of hybrid techniques can prolong surgery time and increase the risk of technical errors. The use of multiple devices may also lead to hardware-related complications, such as irritation or increased inflammation, negatively impacting the recovery process [12].

Figure 8 *- Suspensory device with an interference screw technique. Adapted from [18]*

Tunnel fillers

Tunnel fillers (TF) are a critical advancement in orthopedic surgery, particularly in anterior cruciate ligament (ACL) reconstruction. They are designed to fill bone tunnels created during surgery, ensuring the secure anchoring of grafts or implants, thereby promoting better integration with the surrounding bone and ensuring long-term joint stability [19;20].

Materials used for tunnel fillers vary widely and are selected based on their specific properties that enhance the healing process. Calcium phosphate-based bone cements are commonly used due to their osteoconductive properties, which support new bone tissue growth, aiding in the integration of grafts with the existing bone structure [20]. Polylactide (PLA) granules are also used, recognized for their biocompatibility and high specific surface area, which make them effective in osteoconductive applications [21]. Additionally, silk fibroin-based composite grafts combined with ZnSr-doped β-tricalcium phosphate (β-TCP) have shown promise as bone tunnel fillers, offering enhanced mechanical properties and bioactivity, crucial for bone regeneration and graft integration [19]. Moreover, different types of tunnel fillers provide varied benefits. Silk fibroin-based grafts, when combined with materials like polycaprolactone (Pcl) fibers and β-TCP, represent a cutting-edge approach in promoting tendon-to-bone healing, especially in ACL reconstruction [19]. These composites are designed to mimic the

natural bone environment more closely, thereby promoting faster and more effective osteointegration.

The primary function of tunnel fillers is to provide structural support within bone tunnels, ensuring that the graft remains securely in place. This is vital for maintaining joint stability and the overall success of surgeries like ACL reconstruction. Materials like calcium phosphate bone cements can remodel over time, being gradually replaced by new bone tissue, ensuring seamless integration with the natural bone [20]. The silk fibroin-based composite grafts exhibit favorable swelling properties and a controlled degradation profile, which are essential for adapting to the bone environment and promoting osteointegration [19]. However, tunnel fillers present both advantages and disadvantages. They allow for single-stage revision surgeries by providing immediate stability to the graft, potentially reducing the need for a secondary procedure and thus shortening recovery time [20]. The resorbable nature of materials like PLA granules means they gradually break down and are replaced by natural bone, eliminating the need for future surgeries to remove the filler [21]. Conversely, handling materials such as PLA granules can be technically challenging due to their tendency to interact electrostatically, leading to uneven distribution within the bone tunnel, which may compromise graft integration [21]. Additionally, while materials like calcium phosphate bone cements are promising, their long-term effectiveness and integration in clinical settings require further research [20;19].

Despite the current available alternative, fixation and anchoring issues still exist and are the most significant challenges among the various graft fixation methods [12;14]. These problems are prevalent because they directly impact the stability and longevity of the reconstruction. Inadequate fixation can lead to graft slippage, tunnel widening, and eventual failure, all of which compromise the overall success of ligaments reconstruction. Reasons for prevalence are described in the following table (Table 2):

Table 2 *- Reasons for prevalence of fixation and anchoring problems*

Issue	Explanation
Biomechanical Challenges	Some methods, particularly adjustable-loop devices, are prone to loosening under cyclic loading, leading to gradual loss of tension and stability. This is especially concerning as the "bungee cord effect" observed in these devices can significantly reduce their effectiveness over time [14;11]
Technical Difficulties	The precision required for graft fixation, particularly with cross-pin systems and hybrid techniques, increases the likelihood of errors that can compromise the fixation. Misalignment, improper tensioning, and inadequate graft positioning are all common issues that can lead to suboptimal outcomes [12].
Patient-Specific Factors	Variations in bone quality, graft size, and patient activity levels all contribute to the success or failure of graft fixation. Patients with poor bone density are at higher risk of fixation failure, as their bones may not provide sufficient support for the devices used [11].

1.6. Polycaprolactone (Pcl) as a biomaterial to produce a Tunnel filler

Given the challenges associated with current graft fixation methods - such as graft slippage, inadequate tensioning, and poor osteointegration - innovative solutions like TF present a promising advancement in ACL reconstruction. The TF's design specifically addresses the shortcomings of traditional methods by enhancing fixation strength and promoting better integration with bone tissue.

The procedure with TF involves introducing the filler into the drilled bone tunnel, through which the graft is passed. The subsequent tightening of a screw ensures that the TF applies pressure against the tunnel walls, thereby preventing loosening of both the graft and the screw. This method provides a secure fixation, potentially overcoming the issues seen with interference screws, such as tunnel widening and graft laxity, by

distributing the pressure more evenly and increasing the contact area between the graft and the bone [4]. Moreover, TF can be engineered with a rough surface to improve grip and stability within the graft tunnel (Figure 9). This design contrasts with the smoother surfaces of some traditional grafts, which often fail to provide sufficient anchorage, particularly when cyclic loading occurs [22]. By enhancing the mechanical fixation through this rough surface, TF may reduce the risk of graft slippage and failure, which are common concerns with adjustable-loop devices and other current fixation techniques [4].

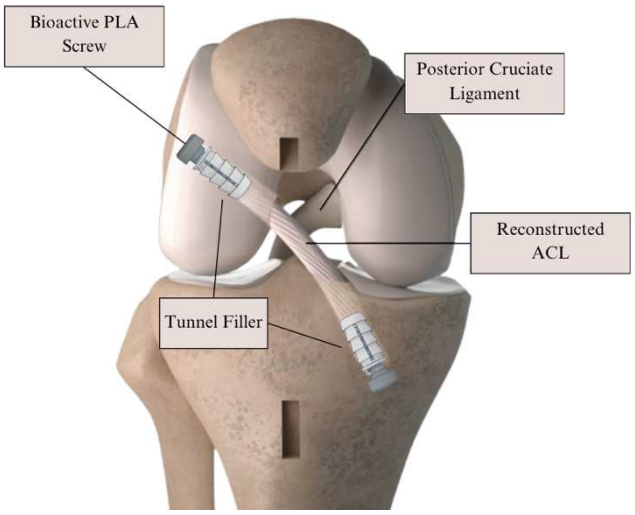

Figure 9 *- Tunnel filler with a bioactive PLA screw as a potential graft fixation problem solver. Adapted from [23]*

1.7. 3D Printing in biomedical applications

3D printing, also known as additive manufacturing, is a transformative technology that creates three-dimensional objects from digital models by adding material layer by layer. This process begins with a digital design, typically created using computer-aided design (CAD) software. The design is then sliced into thin horizontal layers, which the 3D printer uses as a blueprint to deposit material, building the object in a bottom-up approach. The versatility and precision of 3D printing have revolutionized various industries, enabling the production of complex structures that are difficult to achieve with traditional manufacturing methods [24;25].

The applications of 3D printing are vast, spanning industries from aerospace, where lightweight components are essential, to the medical field, where customized prosthetics and implants are becoming increasingly common [26]. The ability to quickly prototype designs and create bespoke solutions has made 3D printing an invaluable tool in modern manufacturing and healthcare [26]. In orthopedics, 3D printing has been particularly impactful, allowing for the creation of custom implants and surgical tools that are tailored to the specific anatomical needs of patients [19]. This level of customization enhances the precision of surgeries and improves patient outcomes, particularly in complex procedures like ACL reconstruction, where tunnel fillers play a critical role [19].

The tunnel fillers used in this context were printed using Pcl, a biodegradable polyester that is particularly well-suited for medical applications due to its unique properties. Pcl is highly favoured in orthopaedic solutions because of its biocompatibility, slow degradation rate, and mechanical characteristics that closely mimic those of human tissue [27]. These attributes make it an ideal material for implants that need to integrate seamlessly with bone and other tissues [27]. The application of Pcl in the production of tunnel fillers highlights the significant advantages of 3D printing in the medical field. This biomaterial not only provides the necessary structural support for the implants, but also promotes bone regeneration and tissue integration, which are crucial for the success of surgeries such as ACL reconstruction [19]. By leveraging 3D printing technology and using materials like Pcl, it becomes possible to create highly customized and effective solutions that significantly enhance surgical outcomes and expedite patient recovery times [19].

1.8. Electrospinning as a coating technique

Electrospinning is a versatile and highly effective technique used to create continuous nanoscale fibers through the application of a high-voltage electric field to a polymer solution or melt. This method is particularly valued for its ability to produce fibers with diameters ranging from the micrometer to nanometer scale, making it ideal for various applications, especially in the biomedical field [28]. The process of electrospinning begins by charging a polymer solution using a high-voltage power supply. As the voltage increases, the solution at the tip of the needle forms a Taylor cone and a

jet of the solution is ejected towards a grounded collector. The solvent in the jet evaporates during this flight, leaving behind solid fibers that accumulate on the collector as a non-woven mat [29].

The applications of electrospinning are broad and impactful, particularly in the creation of scaffolds for tissue engineering, wound dressings, and drug delivery systems [30]. The unique properties of electrospun fibers, such as their high porosity, large surface area-to-volume ratio, and excellent mechanical strength, make them particularly suited for these purposes [29]. In tissue engineering, for instance, the fibrous structure of electrospun mats closely mimics the extracellular matrix (ECM), promoting cell attachment, proliferation, and differentiation, which are essential for successful tissue regeneration [30;4].

One of the significant advancements in the use of electrospinning in orthopedic applications is the incorporation of Pcl electrospun fibers into TF. The integrationof Pcl electrospun fibers as coating envisions not only to improve cell attachment and proliferation but also osteointegration. This is particularly important in ligaments reconstruction, where traditional grafts often suffer from inadequate anchoring within the bone tunnel due to smooth surfaces that do not promote sufficient cellular attachment [4]. The rough, fibrous surface of electrospun Pcl fibers can address this issue by providing a conducive environment for cellular growth, thereby improving the integration of the graft with the surrounding bone tissue and potentially leading to faster and more stable graft fixation [28;29]. Moreover, electrospinning allows for the creation of composite materials, combining different polymers to enhance the functionality of the fibers. For example, coaxial electrospinning can be used to produce fibers with a core-shell structure, where different materials are used for the core and the shell to combine their properties. This technique has been used to fabricate fibers that are mechanically strong and biologically active, making them suitable for more advanced biomedical applications [28].

1.9. Brushite

Brushite (Brh), or dicalcium phosphate dihydrate (DCPD), has been applied in biomedical applications due its biocompatibility, resorbability, and osteoconductivity

[31]. Addiotionally, Brh can act as a coating to enhance cellular attachment and proliferation, which is crucial for effective osteointegration [32]. The resorbable nature of Brh allows it to be gradually replaced by natural bone, ensuring long-term stability and integration of the graft. This property is particularly advantageous compared to traditional fixation methods, where the integration of synthetic materials with bone tissue can be less predictable [32;31]. Brh rough surface promotes better cellular interaction than many current fixation devices, addressing the common issue of inadequate anchorage in smooth-surfaced grafts [33]. Additionally, brushite's ability to be resorbed and replaced by natural bone over time provides a significant advantage in long-term applications, potentially reducing the need for revision surgeries due to graft failure [31].

2. Experimental Procedures

2.1. Materials

In this project, a comprehensive array of materials and equipment was employed to ensure the successful development and testing of the Tunnel Filler. A 3D printer (Flashforge Creator 3) was utilized to create precise models using Pcl filament (Facilan™ Pcl 100 Filament) as the primary material for Tunnel Filler production. During the electrospinning process, Pcl in pellets was employed alongside a syringe pump (NE-1000 One Channel Programmable Syringe Pump, New Era Pump Syringes, Inc.) and an electric potential generator (Genvolt 7000 Series Power Supply) to generate the necessary electric field, with a rotary engine (ASLONG DC MOTOR JGB37-3530-12V-20RPM) being crucial for achieving uniform fiber distribution.Acetone (Carlo Erba Reagents) was used as a solvent for Pcl, and an oven (Memmert) was employed for drying the samples. Surface analysis was conducted using a Scanning Electron Microscope (SEM, Thermo Scientific Phenom Pro), with sample preparation facilitated by a coating machine (Polaron SC7640 Sputter Coater). Material characterization was performed using Fourier-transform infrared spectroscopy (FTIR, PerkinElmer precisely – Spectrum 100), and a texturometer (Texture Analyser TA.XTplus) was employed to assess the mechanical properties of the samples. Calcium chloride (Sigma Aldrich) and sodium dihydrogen phosphate (Sigma Aldrich) were essential for producing brushite.

For cell culture experiments, DMEM culture medium (DMEM high glucose with L-glutamine 500 mL, Gibco, Cat# 41965039) was supplemented with an antibiotic (Antibiotic-antimycotic, 100x, Gibco, Cat#15240-062) and FBS (Fetal Bovine Serum, BioWest, Cat# S181B-500). TrypLE Express Enzyme (TrypLE™ Express Enzyme, 1X, phenol red, Gibco, Cat#12605-028) was used to detach cells from surfaces, while PBS (Phosphate-buffered saline) was prepared using Sodium Phosphate Dibasic (Sigma Aldrich, S3264-500G, ≥98.5%), Potassium Phosphate Monobasic (Fluka, 60220, ≥99.5%), Sodium Chloride (Honeywell | Fluka, ≥99.5%), and Potassium Chloride (Sigma-Aldrich, P5405-500G, ≥99.0%). Resazurin Sodium Salt (Sigma-Aldrich, R7017-5G) was employed as a viability indicator, with assay results measured using a plate reader (Biotek Synergy H1 microplate reader with Gen5 imager software). Fibroblast cells were cultured for biological testing and DMSO (Dimethyl Sulfoxide, CryoSure –

DMSO, 99.9%, USP Grade) serving as a cytotoxic agent and, consequently, positive control for cell culture experiments. Calcein-AM (BioLegend) and Propidium Iodide (PI) (BioLegend) were used for staining live and dead cells, respectively, with visualization carried out using a fluorescence microscope (Axiovert 5 microscope with X-Cite LED fluorescence illumination system). The cell culture processes were conducted in an incubator (Binder CO2 Incubator CB 150).

2.2. Procedures

2.2.1. 3D Printing of the Tunnel Filler

First, the 3D design of the TF was optimized. Existing 3D models were identified and customized using a computer-aided design (CAD) software (ThinkerCAD).

After 3D design optimization, we proceeded to the 3D printing phase. Our aim was to test different printing parameters using Pcl filament. This involved testing different 3D printing parameters, such as layer heights, extrusion temperatures, platform temperatures, printing speeds, extrusion speeds, and infill patterns.

2.2.2. Brushite production using Calcium Chloride and Sodium Dihydrogen Phosphate

To acquire Brushite for our project, we decided to produce it in our laboratory rather than purchasing it. This approach allowed us to ensure the highest quality and purity of the material, as well as to have complete control over the production process.

To produce Brushite, a series of well-defined steps in an existing protocol [34] were followed, which are outlined below:

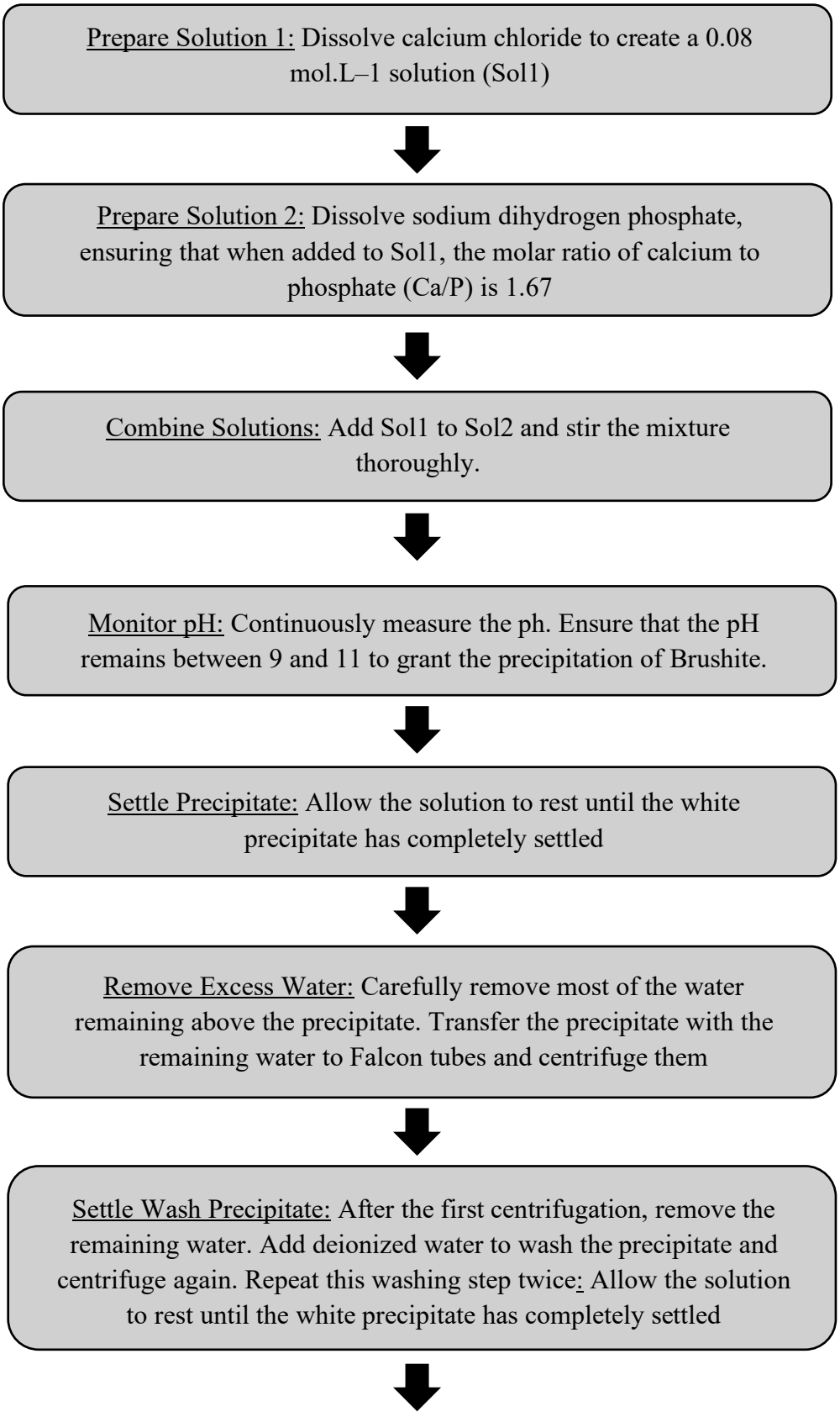
Prepare Solution 1: Dissolve calcium chloride to create a 0.08 mol.L–1 solution (Sol1)
Prepare Solution 2: Dissolve sodium dihydrogen phosphate, ensuring that when added to Sol1, the molar ratio of calcium to phosphate (Ca/P) is 1.67
Combine Solutions: Add Sol1 to Sol2 and stir the mixture thoroughly.
Monitor pH: Continuously measure the ph. Ensure that the pH remains between 9 and 11 to grant the precipitation of Brushite.
Settle Precipitate: Allow the solution to rest until the white precipitate has completely settled
Remove Excess Water: Carefully remove most of the water remaining above the precipitate. Transfer the precipitate with the remaining water to Falcon tubes and centrifuge them
Settle Wash Precipitate: After the first centrifugation, remove the remaining water. Add deionized water to wash the precipitate and centrifuge again. Repeat this washing step twice: Allow the solution to rest until the white precipitate has completely settled

Substitute with Ethanol: Replace the deionized water with 96% ethanol and repeat the washing and centrifugation steps three times

Dry the Precipitate: Transfer the precipitate from the Falcon tubes to a petri dish and dry it in an oven overnight at a maximum temperature of 40°C

By producing Brh in-house, we were able to tailor the synthesis process to meet our specific needs and to fine-tune the properties of the resulting material. This not only provided us with a superior product but also enhanced our understanding of the material's characteristics and behaviour.

2.2.3. Pcl fibers production with electrospinning technique

To start the process, Pcl was first dissolved in acetone at 70ºC. Various Pcl concentrations were tested including 7.5 % and 10% w/v. Then, the solution was transferred to the syringe that, in sequence, were plugged to the syringe pump. The potential difference machine was turned on and settled with the desired voltage. Then, the syringe pump is tuned on with the parameters settled before and Pcl fibers start to coat the TF (Figure 10).

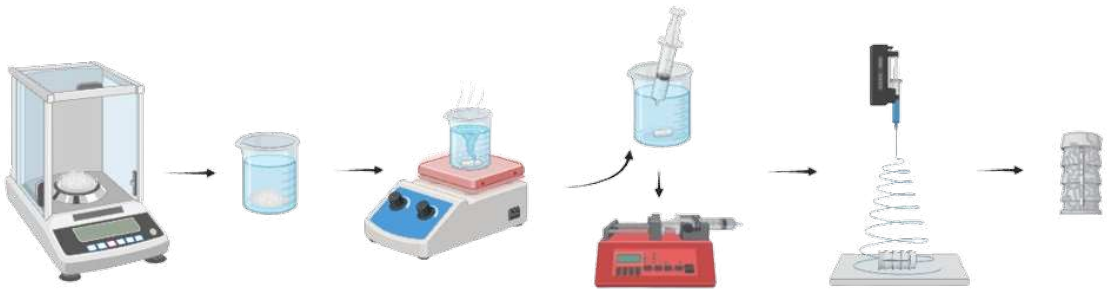

Figure 10 *- Pcl electrospun fibers producing process*

To achieve the best fiber dispersion on the TF, we used a rotary motor with a stick to which the Tunnel Filler was attached, keeping it in constant rotation. The rotary motor operated at a single speed of 30 rpm (Figure 11). Then, time of exposure was optimized.

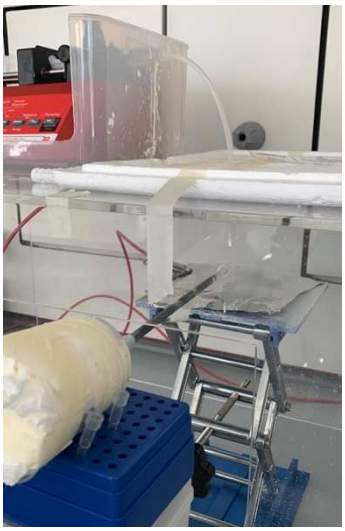

Figure 11 *- Engineered mechanism to produce Pcl electrospun fibers with the best dispersion possible*

2.2.4. Coating Tunnel Fillers with Brushite

Two approaches were tested: (1) combine the Brh with Pcl during the eletrospinning process; and (2) dipping the TF in Brh solutions combined with other components.

The fist approach consisted in adding the brushite (2% - 10% w/v) to the solution during the process of making off the Pcl electrospinning standard solution. Then the whole process is like the described above for the electrospinning with just Pcl

The second approach consisted in coating TF through a dipping process. Firstly, Brh was combined with several compounds, including PVA, ethanol, gelatin, deionized water, and Pcl solutions. Two different of Brh concentrations were tested (5% and 10% w/v) and the dipping time was optimized for 30 seconds. After dipping, the TF was placed in an oven at 40ºC to dry for approximately 2 hours (Figure 12).

After the drying period, the dipping process was complete. The formulations were defined as followed:

- Control Tunnel Filler (untreated) - TF
- Tunnel Filler with electrospun Pcl fibers - TFE
- Tunnel Filler with electrospun Pcl fibers and brushite coating – TFE + Brh

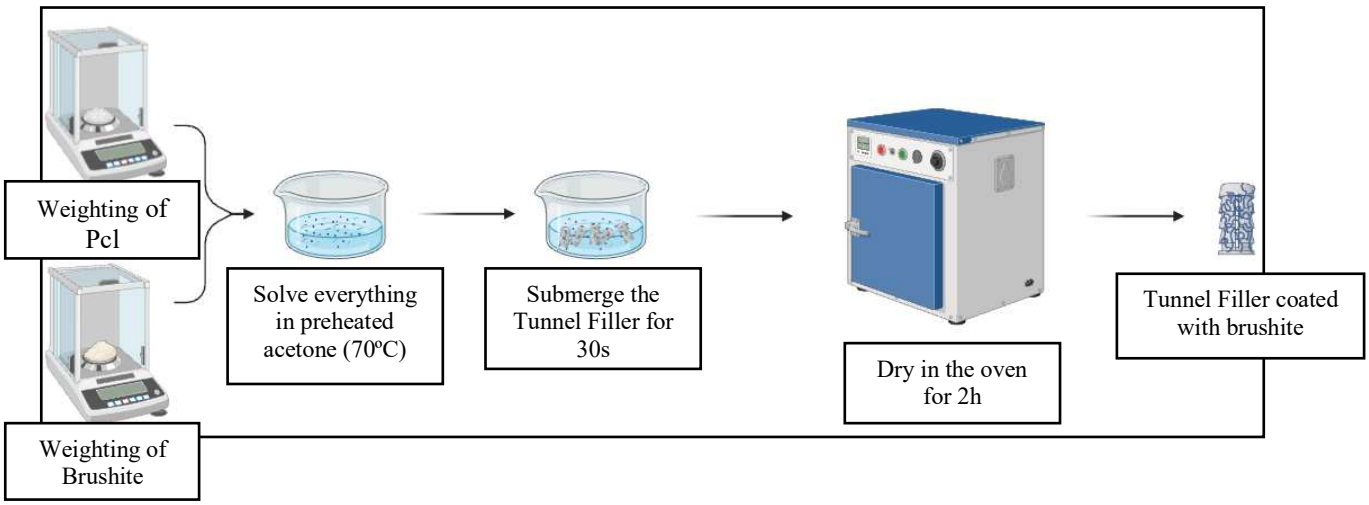

Figure 12 *-Brushite coating through a dipping process*

2.3. Characterization Techniques

2.3.1. SEM analysis

To analyse all the steps at a microscopic level, we used a SEM. TF was cut it into smaller pieces to make it available for microscopic analysis.

To prepare these pieces for SEM analysis, we used PINs with carbon fiber tape to attach the pieces to the analysis platform. These PINs must undergo a thin coating process with metals, specifically gold and palladium. This step is necessary because Pcl is not an electron conductor. The electrons ejected by the SEM need to interact with the sample and be reflected to the SEM's detectors. By coating the sample with conductive metals, we ensure proper electron reflection.

Using the Secondary Electron Detector (SED) mode of the SEM, we could then analyse the surface of our sample. This analysis allowed us to assess the quality of the Tunnel Filler and its coating at a high resolution, providing valuable insights into the microscopic structure and surface characteristics (Table 3).

Table 3 *- SEM analysis parameters*

Parameter Category	Specific Parameter	Value/Setting
System	Acquisition voltage	5 kV
	Beam Density	Point
	Detector	SED

Live	Averaging	High
	Scan Size	1440 x 900
Acquisition	Averaging	High
	Scan Size	3840 x 2400

2.3.2. FTIR Spectroscopy analysis

To characterize the Tunnel Filler, we utilized Fourier Transform Infrared Spectroscopy (FTIR) tests. FTIR is an analytical technique used to identify organic, polymeric, and in some cases, inorganic materials. The method works by measuring the absorption of infrared radiation by the sample material at different wavelengths. The resulting spectrum represents the molecular fingerprint of the material, allowing for identification and characterization based on known reference spectra.

To perform these tests, the TF was cut into smaller pieces to fit the FTIR machine's sensor. After resizing, the samples were placed on the sensor for analysis. Three independent conditions (n = 3) were tested to ensure high-quality and reliable results.

After obtaining the FTIR spectra, the next step was to compare the results with established reference data. By matching our results with tabled data, we ensured the accuracy and correctness of our characterization.

2.3.3. Swelling Test

To evaluate the liquid absorption capacity of the TF, a series of swelling tests were conducted (Figure 13). This experiment was designed to determine how the TF, in its various conditions, interacts with a physiological solution, mimicking the environment it would encounter *in vivo*.

Each piece was carefully weighed to obtain its initial weight, which was recorded for subsequent comparison.

The prepared Tunnel Filler pieces were placed into well plates, with each condition separated into distinct wells. The wells were then filled with a phosphate-buffered saline (PBS) solution, chosen for its similarity to the body's natural fluids. These

well plates were then placed in an orbital shaker, where the rotation speed was kept low to gently agitate the solution, ensuring consistent exposure of the Tunnel Filler pieces to the PBS. The temperature was maintained at a physiological 37°C to replicate the conditions within the human body.

At predetermined time points, such as 1, 2, 4, 8, 24, 48 and 72 hours, the Tunnel Filler pieces were removed from the PBS solution and gently dried to remove excess surface liquid. Each piece was then reweighed to measure its weight after swelling. This process of drying and weighing was repeated for all the time points required by the test protocol, allowing for the calculation of the swelling ratio and analysis of how each Tunnel Filler condition absorbs and retains liquid over time. The following equation was uses to calculate swelling ratio [19]:

$$\text{Swelling ratio } (\%) = \left[\frac{(m_w - m_i)}{(m_i)}\right] \times 100\%$$

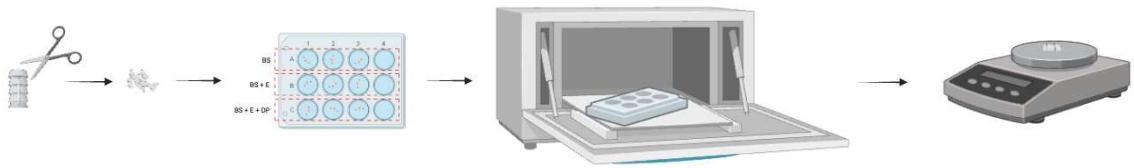

Figure 13 *- Swelling process*

2.3.4. Mechanical Properties Tests

To test the mechanical properties of the TF, two types tests were conducted: tension and compression tests. For both mechanical tests, it was done 5 tests with independent samples for each formulation (n = 5). For all the tests a pre-load of 0.05N was used.

2.3.4.1. Tension Test

To proceed with the tension test, it was necessary to attach the claws to the equipment. These claws are what hold the TF in place during the test (Figure 14).

Given the difficulty of holding an entire TF with the available claws, TF was cut vertically into four independent pieces, where each piece had 25 x 7 mm for its dimensions (Figure 14).

During the tests, it is important to ensure that the initial height of the movement is consistent in every test to increase the precision of the process. It is equally important to maintain the same position for each sample in the claws.

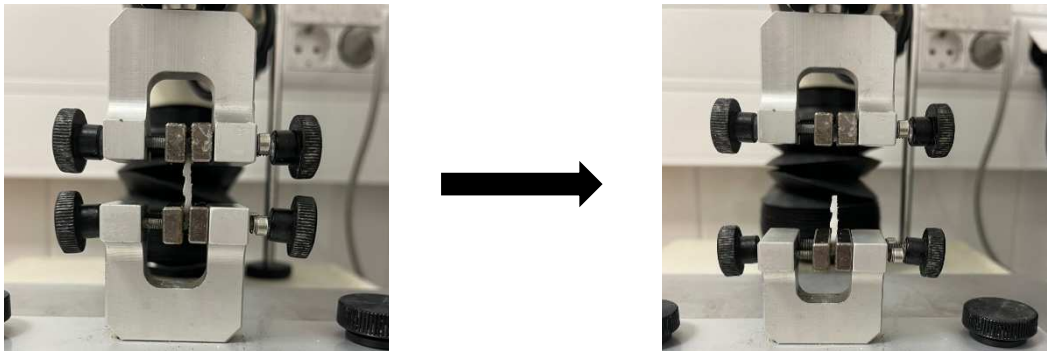

Figure 14 *- Tension test*

2.3.4.2. Compression Test

In this test, the complete TF was used (Figure 15). Once the setup was complete, all the parameters were configured, and everything was ready to proceed with the compression tests.

To ensure the quality and reliability of the tests, it is important to ensure that the initial height of the movement is consistent in every test to increase the precision of the process.

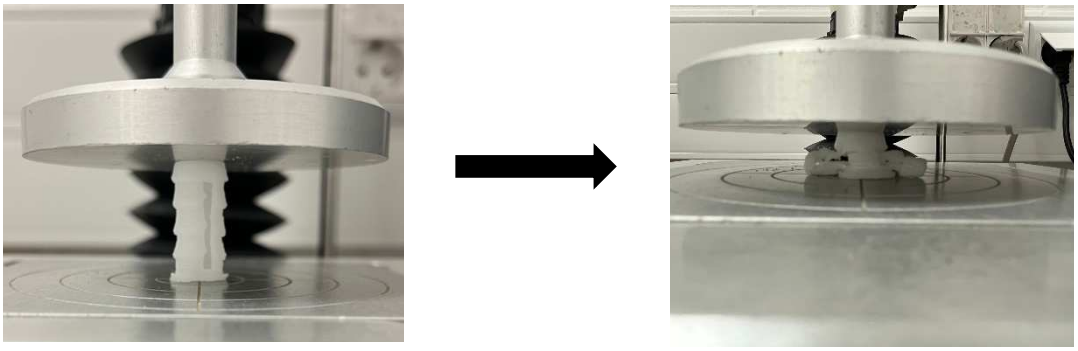

Figure 15 *- Compression test*

2.3.5. *In vitro* cell culture - Cytotoxicity Tests

2.3.5.1. Alamar Blue assay (Metabolic activity)

The Alamar Blue assay is a widely used method for assessing cell viability and cytotoxicity. It relies on the reduction of resazurin, a non-toxic, cell-permeable dye, into resorufin, a highly fluorescent compound, by metabolically active cells. Resazurin (7-hydroxy-3H-phenoxazin-3-one 10-oxide) serves as an indicator of cell viability, as its reduction to resorufin occurs in proportion to the number of living cells. This property makes the Alamar Blue assay a reliable tool for evaluating the biocompatibility of materials, including biomedical implants and tissue scaffolds [35].

An indirect contact assay was performed (Figure 16). Human dermal fibroblasts (HDFs) were used. To prepare the leachate solution, samples were immersed in complete DMEM medium for 24 h. A suspension of 10^4 cells/ml was used for cell seeding in a 96 well plates and left in a CO_2 incubator (BINDER GmbH, Tuttlingen, Germany) for 24 h. Afterwards, the leachate solution was added and the timepoints testes were 24 hours, 48 hours and 72 hours. To validate the tests, DMSO was used as a positive control, while untreated cells served as the negative control.

Following the incubation period, the Alamar Blue reagent is added to the culture medium in each well, at a volume of 10% of the total culture medium volume. The plates are returned to the incubator, where the cells are allowed to metabolize the resazurin into resorufin over a period of 2 hours. During this time, viable cells reduce the resazurin, leading to an increase in fluorescence or absorbance, which can be measured to quantify cell viability. After the incubation with the Alamar Blue reagent, the culture medium is collected, and its fluorescence is measured using a plate reader with an excitation wavelength of 530-560 nm and an emission wavelength of 590 nm. The intensity of the fluorescence correlates directly with the number of viable cells present, providing a quantitative measure of the material's biocompatibility.

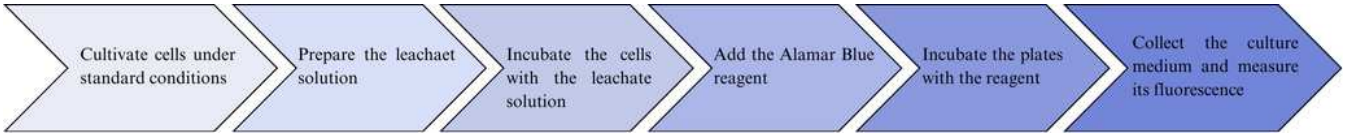

Figure 16 *- Alamar Blue test step by step*

2.3.5.2. Live/Dead Test

The Live/Dead assay is a fluorescence-based method frequently used to evaluate cell viability and cytotoxicity in various biological studies. This assay uses two dyes: Calcein-AM and Propidium Iodide (PI). Calcein-AM is a non-fluorescent, cell-permeable dye that is hydrolyzed by intracellular esterases in live cells. On the other hand, PI is a red fluorescent dye that cannot penetrate intact cell membranes but readily enters cells with compromised membranes, binding to DNA and staining the nuclei of dead cells. The dual staining allows for a clear distinction between live (green) and dead (red) cells [36;37;19] (Figure 17).

To perform the Live/Dead assay, indirect contact assay was performed as mentioned before. After culturing, the medium is aspirated, and the cells are gently washed with phosphate-buffered saline (PBS) to remove any remaining culture medium. A staining solution is then prepared by diluting Calcein-AM to a final concentration of 2 μM and Propidium Iodide to a final concentration of 20 μg/mL in PBS. The cells are incubated with this staining solution at 37°C for 20-30 minutes, ensuring the process is conducted in the dark to prevent photobleaching of the dyes [19].

Post incubation, the staining solution is removed, and the cells are washed again with PBS to eliminate any excess dye. The stained cells are then examined using a fluorescence microscope equipped with appropriate filters for green and red fluorescence. Fluorescence microscopy images are captured to analyze and quantify the live (green) and dead (red) cells.

The Live/Dead assay also serves as a complementary method to the Alamar Blue assay in confirming cell viability. While Alamar Blue indicates metabolic activity, which suggests but does not always guarantee cell viability, the Live/Dead assay provides direct visual evidence of cell viability through the staining of live and dead cells. By using both assays, a more comprehensive assessment of the material's biocompatibility can be achieved, ensuring that the cells not only maintain metabolic activity but also remain structurally intact and viable.

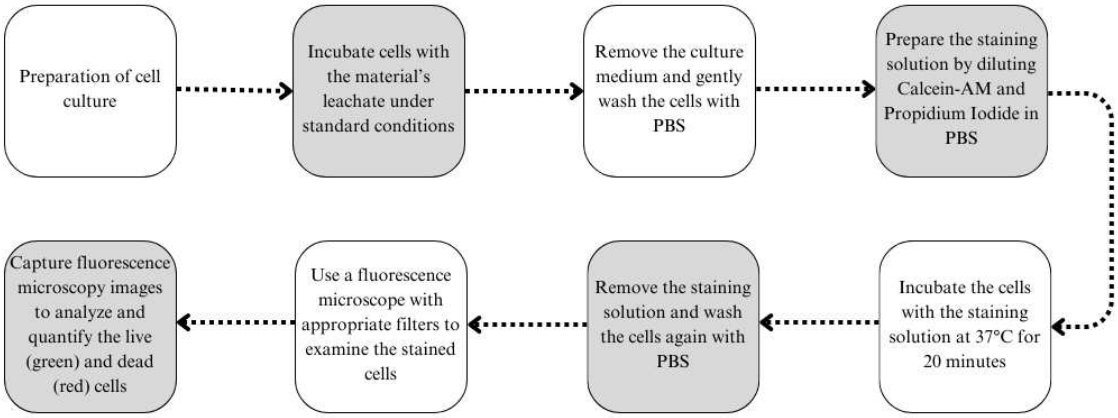

***Figure 17** - Procedure to perform Live/Dead test*

3. Results and Discussion

3.1. Fabrication and Coating Processes

In this section, we present the outcomes of the TF fabrication, which involved three key processes: 3D printing, electrospinning of Pcl fibers, and the application of a Brh coating.

3.1.1. 3D printing

The Tunnel Filler was first created using a 3D printer [Flashforge Creator 3] with PCL filament [Facilan™ Pcl 100 Filament]. The 3D printing process aimed to produce a structurally stable scaffold with precise dimensions.

First, it was mandatory to reach to the ideal printing parameters of the Pcl filament. Through a series of trials, where it was tested many different parameters, it was concluded that the ideal printing parameters were the following:

- Machine type: Flashforge Creator 3
- Layer heigh: 0.3 mm
- Shell count: 3
- Infill: 15%
- Infill format: Hexagonal
- Printing speed: 10 mm/s
- Travel speed: 100 mm/s
- Extrusion temperature: 110 ºC
- Platform temperature: 35 ºC

After reaching the desired printing parameters, various types of possible TF were printed to see which one fits better to the needs of the final goal (Figure 18).

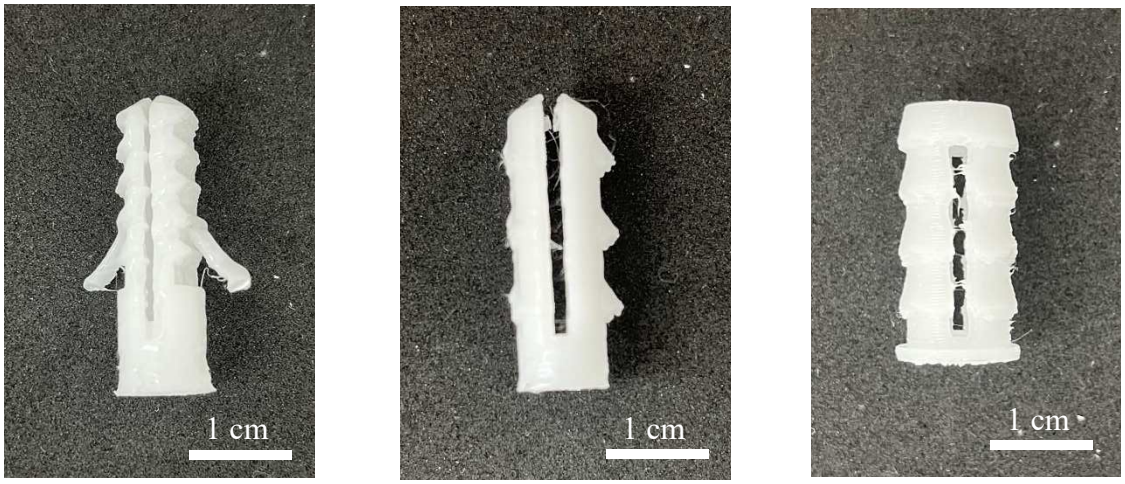

Figure 18 *- Various formats for Tunnel Filler*

Among the various types of TF, it was necessary to select the most suitable option based on several key criteria. To finalize the design, several crucial aspects were identified as requirements for the final TF:

- **Ease of printing**: A 3D model with a compact, solid structure is significantly easier to print compared to designs with complex or "suspended" elements. The simpler, compact design reduces the risk of printing errors and streamlines the manufacturing process.

- **Application-friendly design**: A unique and compact TF design is more reliable for practical application. Since it consists solely of the core body, the TF is easier to use. All that is required is selecting the correct hole diameter to fit the chosen TF, making the application process straightforward and efficient.

- **Robust yet flexible body**: The primary purpose of the TF is to be inserted into a bone tunnel, where it should create consistent pressure against the tunnel walls to improve graft fixation when applied alongside an interference screw. To achieve this, the TF must be strong enough to withstand certain forces without reaching a critical deformation point. Simultaneously, it must possess enough flexibility to deform slightly when the graft and interference screw are applied, ensuring adequate pressure is exerted on the bone tunnel walls for secure fixation (Figure 21).

After careful evaluation, it was selected the model that best met the settled requirements and proceeded to scale up the printing process. Each piece took approximately 45 minutes to print (Figure 19).

Figure 19 *- Final Tunnel Filler design*

During this phase, we encountered several challenges with Pcl filament. Controlling the temperature changes of Pcl proved to be quite difficult. In 3D printing, layers are built one on top of the other, and each underlying layer needs to be nearly dry before adding the next one. With Pcl, each layer required significant drying time, which considerably delayed the overall printing process. To address this issue and reduce printing time, we began printing two pieces simultaneously. This strategy not only expedited the process but also improved the quality of our TF. By optimizing our approach, we successfully increased our production rate and achieved higher quality prints (Figure 20).

Figure 20 *- 3D printing process of the Tunnel Filler*

The bone tunnel in ligaments reconstruction is a carefully crafted channel within the femur and tibia, designed to replicate the natural path and attachment sites of the ligaments [38]. This tunnel is crucial for guiding and securing the graft, ensuring that it functions naturally within the knee joint. The tunnel's dimensions are typically 7 to 10 mm in diameter, with the length of the femoral tunnel usually around 30 to 40 mm and the tibial tunnel extending to match the graft's requirements [38;39]. These dimensions are selected to closely match the original anatomy of the ligament, which is essential for the success of the reconstruction [38].

Recognizing the importance of this precise environment, the TF has been specifically engineered to fit and function within these bone tunnels. The TF is designed to seamlessly integrate into the tunnel, filling any voids and providing essential support during the healing process. The use of a 3D printing process allows to tailor the Its dimensions aiming to enhance the fixation of the graft, ensuring that it remains securely in place as it incorporates into the bone [39].

Regarding the dimensions of the TF, its length has been specifically tailored for cases where it is used in conjunction with a screw. In such cases, the screw's head remains outside the TF, resulting in a total length of 35 cm. The width of the TF, approximately 11 mm, is determined by both the dimensions of the screw used and the thickness of the TF’s walls. These dimensions can be carefully designed to be perfectly adjustable to fit within the bone tunnel when necessary, using 3D printing.

Final dimensions of the Tunnel Filler:

- Length: 25 cm
- Width: 11 mm

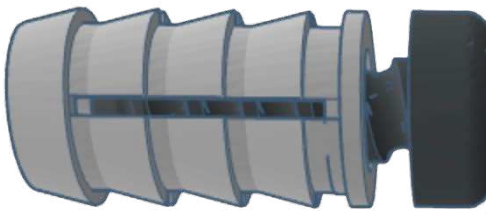

Figure 21 *- TF with BioScrew*

3.1.2. Electrospinning Fibers

TF was coated with electrospun Pcl fibers using a syringe pump [New Era Pump Syringes, Inc.] and an electric potential generator [Genvolt] aiming to obtain a suitable architecture for osteointegration [40].

Initially, Pcl electrospinning was optimized, and different conditions were tested (Table 4).

Table 4 *- Some of the electrospinning tested parameters*

TEST	[PCL] (W/V)	RATE (ML/MIN)	VOLTAGE (KV)	EXPOSURE TIME (S)	NOZZLE (G)
T1	7,5%	20	20	40	20
T2	7,5%	20	23	40	20
T3	10%	20	20	40	20
T4	10%	20	23	40	20

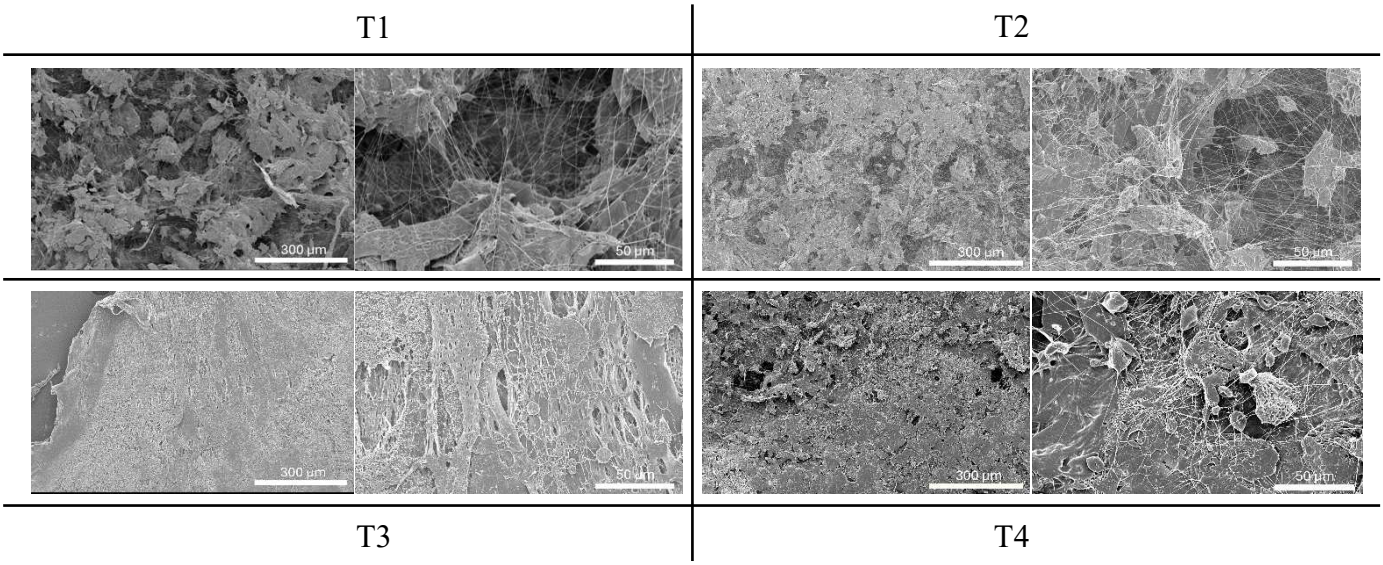

Figure 22 *- SEM images from T1, T2, T3 and T4 electrospinning tests*

Analyzing the SEM images (Figure 22), it is evident that the concentration of Pcl plays a significant role in determining the density of the fibers produced. As the Pcl concentration increases, the fibers become denser and more closely packed. Additionally, increasing the flow rate of the syringe pumps also leads to denser fiber production. However, when the applied potential difference (voltage) is increased, the density of the fibers decreases, resulting in more spaced-out and less compact fiber structures. Knowing this, and being concerned of the requirements for the TF desired result, the choose electrospinning parameters were the ones applied in T2:

Electrospinning Final Parameters:

- [Pcl] = 7,5% w/v
- Voltage: 23kV
- Extrusion rate: 20 μL/min
- Nozzle diameter: 20 G
- Time of exposure: 40 s

The electrospun Pcl fibers exhibit a high surface area-to-volume ratio, significant porosity, and flexibility, making them particularly suitable for biomedical applications such as tissue engineering, wound healing, and drug delivery systems [34]. One of the key characteristics of Pcl electrospun fibers is their ability to enhance cell adhesion and provide a scaffold that supports tissue integration [41]. Additionally, the flexibility of Pcl fibers should allow them to conform closely to irregular surfaces, further improving their ability to integrate with surrounding tissues [42].

3.1.3. Brushite coating

The production of brushite involved a precipitation reaction, achieved by mixing calcium chloride and sodium dihydrogen phosphate. The resulting product from this reaction was a fine and white powder (Figure 23). When comparing brushite to other ceramics like hydroxyapatite, β-tricalcium phosphate (β-TCP), and calcium sulfate, each material offers unique benefits for bone regeneration. HAp is highly osteoconductive and mimics bone mineral content, but its slow resorption makes it more suitable for long-term applications [43;44]. β-TCP resorbs more quickly, promoting faster bone regeneration,

but it has weaker mechanical properties [45]. Calcium sulfate resorbs rapidly, potentially hindering full bone regeneration [45]. In conclusion, brushite appear to be the best balance between bioactivity, moderate resorption, and ease of production, making it good for bone ingrowth and graft fixation [43;44].

Figure 23 *- Macroscopic view of laboratory produced brushite*

The characteristics of the produced brushite powder, observed through SEM images, align well with the findings reported in the literature (Figure 24). Brushite typically exhibits brittle fracture behavior, which makes it suitable for applications where mechanical loading is minimal [31]. Its porous nature, as commonly noted in the literature and in the produced powder, facilitates resorption and encourages bone ingrowth, which is vital for biomedical applications such as bone scaffolding [32]. Additionally, the SEM analysis revealed plate-like crystallite structures, which are characteristic of brushite and contribute to its rapid dissolution and osteoconductive properties in physiological environments [31;32]. These traits make brushite ideal for applications requiring gradual material resorption and bone regeneration support [32].

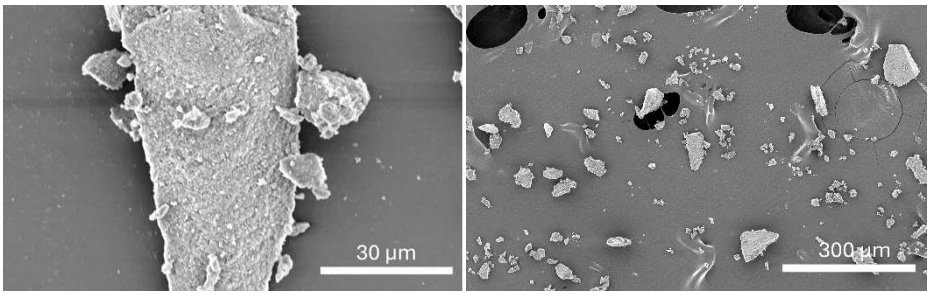

Figure 24 *- Microscopic view of Brushite*

Subsequently, Brh was added to Pcl solution at various concentrations. However, regardless of the concentration, the resulting solution was thicker and frequently clogged the syringe needle, resulting in non-production of fibers during electrospinning process. Therefore, a dipping process was used. The experimental tests for dipping involved various solutions such as PVA, Gelatine, Ethanol, Deionized Water, and Acetone with Pcl, all of which had brushite dissolved in them. The dipping process was tested both before and after adding the electrospun Pcl fiber. In the end, the solution with Pcl dissolved in acetone demonstrated the best results, showing the most effective brushite dispersion and adhesion, meeting our experimental objectives.

To optimize the dipping solution, we tested brushite concentrations of 5% and 10% w/v to determine the ideal concentration. Following extensive testing, the parameters for the final dipping solution were established as follows:

- Acetone Volume: 50 mL
- Pcl Concentration: 2.5% w/v
- Brushite Concentration: 5% w/v

3.2. Material Characterization

3.2.1. SEM analysis of Tunnel Filler morphological properties

The SEM analysis of the three conditions (Figure 25) - TF, TFE, and TFE + Brh - reveals distinct differences in surface morphology that correlate with their processing.

The TF condition, consisting solely of 3D printed Pcl, displays a relatively smooth surface (Figure 25, (A)). Pcl's well-documented biocompatibility and mechanical properties make it suitable for a variety of biomedical applications. However, the smooth surface observed here could limit cell attachment and proliferation, which are crucial for effective tissue regeneration [46]. This aligns with findings in the literature where smoother surfaces generally provide fewer binding sites, potentially reducing scaffold effectiveness in promoting cellular activities [27].

The incorporation of electrospun Pcl fibers in the TFE condition significantly enhances surface roughness, mimicking the ECM (Figure 25, (B)). This fibrous architecture is advantageous for cell attachment, spreading, and proliferation—critical aspects of tissue regeneration. The increased surface area and topographical features provided by the electrospun fibers make the TFE condition more prone for cell-material interactions, as supported by research on electrospun scaffolds, which emphasize their role in enhancing cellular responses [46;47].

Adding a brushite coating in the TFE + Brh condition introduces a rougher, more complex surface. Brh, enhances the scaffold's potential for bone tissue engineering [47]. SEM images (Figure 25, (C)) show that the brushite coating adds structural complexity, potentially improving the scaffold's ability to support bone cell attachment and proliferation. However, the non-uniformity of the coating observed in some regions could affect the scaffold's overall mechanical properties and consistency, a challenge noted in studies involving coated scaffolds [48].

When comparing the three conditions, it is evident that the addition of electrospun fibers and brushite coating significantly alters the scaffold's surface characteristics. While the TF condition provides a mechanically robust scaffold, the TFE and TFE + Brh conditions offer the possibility to enhance its bioactivity due to increased surface roughness and bioactivity of Brh. This variation in surface morphology underscores the importance of customizing scaffold designs to specific applications, whether for soft tissue engineering or bone regeneration [27].

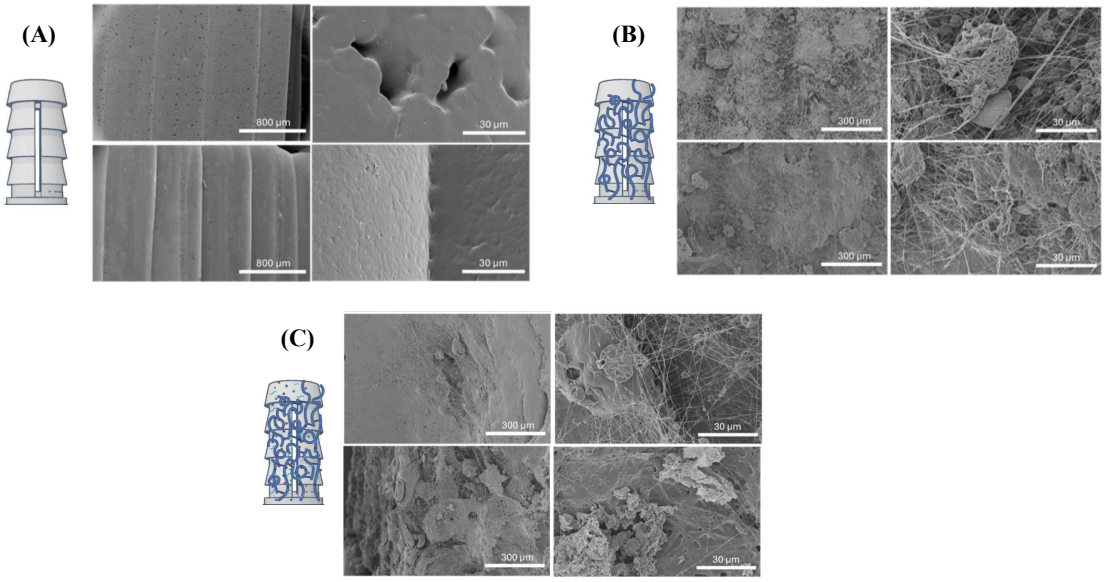

Figure 25 *- SEM images of the TF (A), TFE (B) and TFE + Brh (C) conditions*

3.2.2. FTIR

The FTIR spectra for the all the TF samples (Figure 26) – TF, TFE and TFE + Brh - show distinct peaks that correlate with the materials' compositions (Table 5). The TF sample, consisting purely of Pcl, exhibited major peaks such as O-H stretching vibration at ~3300 cm^{-1}, C-H stretching at ~2940 cm^{-1}, and C=O stretching at ~1720 cm^{-1}. These peaks are characteristic of Pcl, confirming the presence of its polymer backbone [27;49]. The TFE sample, which includes both 3D printed Pcl and electrospun Pcl fibers, retained these peaks but showed a slightly more pronounced O-H peak. [51]. Lastly, the TFE + Brh sample showed similar Pcl-related peaks, along with new peaks around ~1100 cm^{-1}, indicating the successful incorporation of Brh through the phosphate groups' P-O stretching vibrations [50].

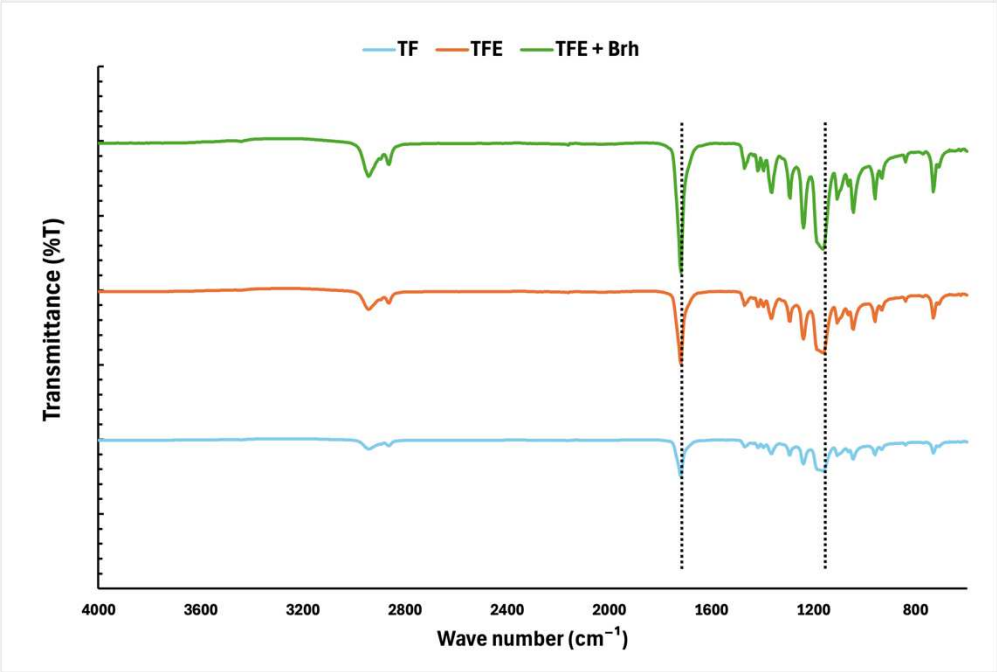

Figure 26 *- FTIR graphic conclusions*

Table 5 *- Results from FTIR tests*

Sample	*Wavenumber ((cm^{-1}))*	*Observed Peak*	*Interpretation*
TF	~2940	C-H stretching vibrations	Confirms the presence of methylene groups in the Pcl polymer backbone [49]
	~1720	Carbonyl (C=O) stretching vibration	Characteristic peak for ester groups in Pcl, indicating the polymer structure [52]
	~1500 - 1000	C-O stretching and C-H bending vibrations	Confirms the presence of ester and alkyl groups in Pcl [27]
TFE	~2940	C-H stretching vibrations	Consistent with the Pcl polymer backbone, unaffected by the electrospun fibers. [49]
	~1720	Carbonyl (C=O) stretching vibration	Similar intensity, indicating retained ester linkages post-electrospinning. [53]

	~1500 - 1000	C-O stretching and C-H bending vibrations	Slight changes due to fiber morphology differences introduced by electrospinning. [49]
TFE + Brh	~2940	C-H stretching vibrations	The Pcl organic backbone remains intact, unaffected by Brushite.
	~1720	Carbonyl (C=O) stretching vibration	Possible subtle changes due to interactions with Brushite, but Pcl structure is maintained.
	~1100 - 1000	New peaks for P-O stretching	Characteristic of phosphate groups from Brushite, confirming its presence on the material surface. [54]

The FTIR analysis confirms that the structural integrity of Pcl remains consistent across all samples, as evidenced by the persistent C-H and C=O stretching peaks [27] (Table 5). The presence of electrospun Pcl fibers in the TFE sample introduces minor changes in the FTIR spectrum, particularly a slightly more intense O-H stretching peak. This increase is likely due to the larger surface area provided by the electrospun fibers,

which can lead to more significant moisture adsorption—a common occurrence noted in literature when using electrospun materials to enhance surface properties without altering the bulk chemical structure of the material [51;53].

The addition of Brushite in the TFE + Brh sample results in noticeable changes in the FTIR spectrum, particularly the appearance of new peaks around ~1100 cm^{-1}, corresponding to the phosphate groups' P-O stretching vibrations. The successful incorporation of Brushite in the TFE + Brh sample is further supported by the increased intensity of the O-H stretching peak, which is consistent with Brushite's hydrophilic nature [48]. The comparison with the literature confirms that the FTIR results for the TFE + Brh sample are consistent with expectations for a Pcl-based material enhanced with Brushite. The spectrum verifies the successful integration of Brushite without compromising the structural integrity of Pcl, suggesting that TFE + Brh is a promising material for applications requiring both mechanical support and biological activity, such as bone tissue engineering and regeneration [50;52].

3.2.3. Swelling test

The results of the swelling tests (Figure 27) demonstrate differences in the swelling behavior of the various sample compositions, providing insight into how each formulation responds to the PBS absorption.

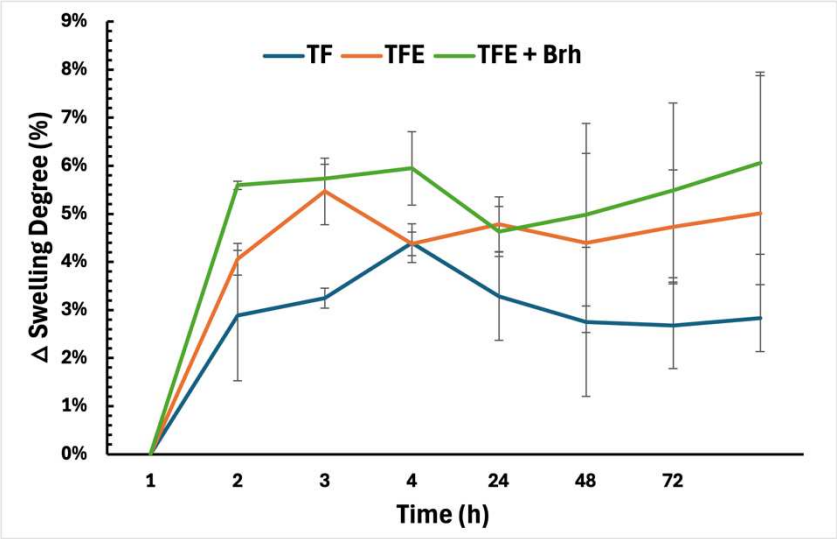

***Figure 27** - Swelling test results*

The TF sample showed an initial swelling of 2.89% ± 1.36% after 2 hours, increasing slightly to 3.25% ± 0.21% after 4 hours, with minimal fluctuations, thereafter, indicating a near-equilibrium state and consistent swelling behavior (low standard deviations of and). The sample with added electrospinning fibers (TFE) exhibited more pronounced swelling, reaching 4.06% ± 0.33% after 2 hours and 5.47% ± 0.69% after 4 hours, suggesting increased hydrophilicity or porosity. The sample with both electrospun fibers and brushite particles (TFE + Brh) showed the highest swelling, at 5.59% ± 0.09% after 2 hours and 5.74% ± 0.29% after 4 hours, with very low variability, indicating a uniform and enhanced liquid absorption capacity.

These results align well with existing literature, confirming that electrospinning fibers and brushite coatings can increase the flexibility and swelling capacity of polymers [42]. The stabilization of swelling after the initial hours indicates that the material reaches a near-equilibrium state, which is important for applications requiring predictable and stable performance over time.

Regarding the application in the body, the swelling observed in the TFE + Brh sample, reaching 5.74% ± 0.29%, is within a reasonable range for certain biomedical applications. According to *Li et al.* (2014) [55], materials used in biomedical applications must carefully balance swelling capacity to ensure they provide adequate support without compromising the surrounding tissue structures. The swelling observed in the TFE + Brh sample is moderate, which suggests that it could be suitable for applications where a certain degree of swelling is necessary to fill spaces or gaps.

However, it's important to highlight those potential sources of error, such as inaccuracies in weighing or inconsistent drying of the samples, could have influenced the measurements. Despite these possible errors, the findings suggest that the formulations used in this study achieved suitable swelling performance. this application.

3.3. Mechanical properties

3.3.1. Tension test

The mechanical properties of the TF, TFE, and TFE + Brh were evaluated through tensile tests (Figure 28 and table 6). The TF sample demonstrated an Ultimate Tensile

Strength (UTS) of 6.94 ± 1.10 MPa and a failure strain of 14.91%, suggesting a moderate capacity to withstand tensile forces with good ductility. The yield stress was 5.47 ± 0.50 MPa, indicating when the material begins to deform plastically. In comparison, the TFE sample showed improved mechanical properties, with a UTS of 7.64 ± 0.63 MPa and the same failure strain of 14.91%. This indicates that the addition of the electrospinning coating enhances the tensile strength without sacrificing flexibility. The yield stress of TFE was 6.16 ± 0.70 MPa, slightly higher than TF, suggesting better performance under stress. On the other hand, the TFE + Brh sample, showed a UTS of 7.02 ± 0.90 MPa and a failure strain of 12.74%, with a lower yield stress of 4.61 ± 0.52 MPa.

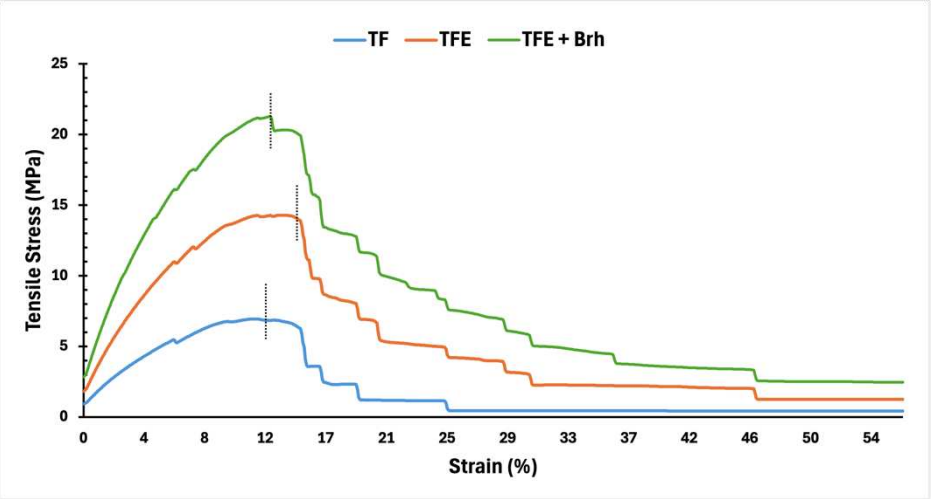

Figure 28 *- Tension mechanical test graphic results*

When considering the use of these TF in ligaments reconstruction, particularly as a support during the initial recovery phase, it's important to recognize that their role isn't to replicate the full mechanical load-bearing capacity of the native ligament. Instead, the primary objective of the TF is to enhance the anchoring and fixation of the graft during the critical early weeks post-surgery. This period is when the graft is most vulnerable, and the surrounding bone is still integrating with the graft tissue.

The native ACL can withstand forces up to approximately 2160 N [56;57], but the initial fixation of grafts typically requires much lower forces, usually ranging between 100-500 N, depending on the biological healing phase and the type of fixation used [43;45]. The mechanical properties of the Tunnel Filler, particularly the TFE formulation,

suggest that it could effectively contribute to stabilizing the graft by providing additional support and anchoring in the bone tunnel, thus promoting better bone growth and reducing the risk of graft loosening.

3.3.2. Compression test

The compression mechanical test results for the TF samples - TF, TFE, and TFE + Brh - provide a comprehensive view of their structural behavior under compressive forces (Figure 29 and table 6). The TF sample exhibited an Ultimate Compressive Strength (UCS) of 9.10 ± 2.83 MPa, with a failure strain of 7.77% and a yield stress of 8.96 ± 1.07 MPa. These values indicate that while the TF formulation has moderate strength, it shows limited plastic deformation before failure, suggesting that it may be relatively brittle under compressive loads (Table 6).

The TFE sample, enhanced with an excipient, showed a slight improvement in UCS to 9.10 ± 2.4 MPa, with a reduced failure strain of 7.27%. The yield stress significantly increased to 9.10 ± 2.13 MPa, indicating that the addition of the electrospun Pcl fibers improves the material's strength and ability to maintain its structural integrity under stress. However, the decrease in failure strain suggests that this formulation is even more brittle than the TF sample, which could be a limitation in applications requiring flexibility.

On the other hand, the TFE + Brh sample, which includes both an excipient and a plasticizer, demonstrated the highest UCS at 10.63 ± 0.16 MPa and a failure strain of 7.71%. The yield stress was also higher at 10.63 ± 0.39 MPa, reflecting a formulation that is both strong and capable of withstanding substantial compressive forces. The slight increase in failure strain compared to TFE suggests that the addition of brushite not only enhances compressive strength but also slightly improves the material's capacity to deform before failure, which could be beneficial in dynamic environments.

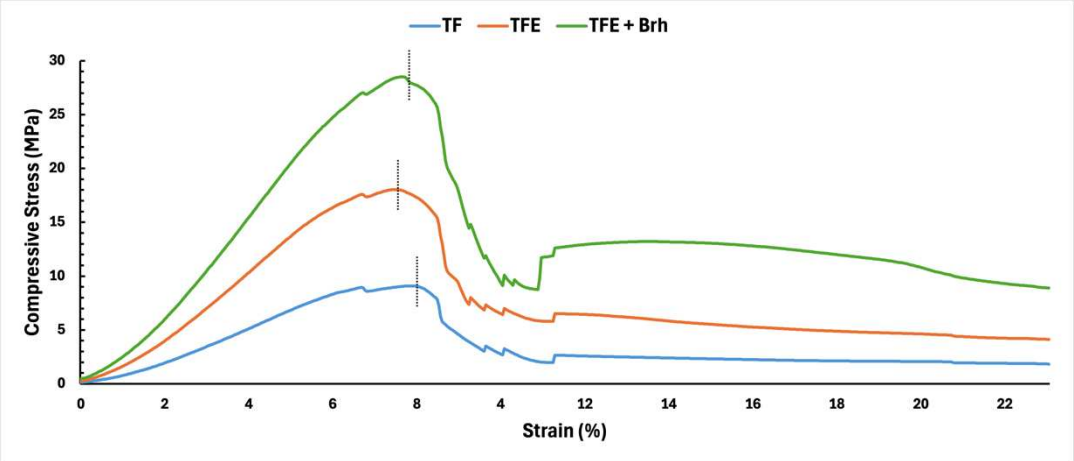

Figure 29 *- Compression mechanical test graphic results*

When considering the application of these Tunnel Fillers in ACL reconstruction, the mechanical properties under compressive loads are particularly important. The role of the Tunnel Filler is not to endure the full spectrum of forces experienced by a fully functional ACL but to provide essential support during the early recovery phase, particularly in enhancing the fixation and anchoring of the graft. According to the literature, ACL grafts typically experience significant forces during the healing process, with ultimate loads to failure for grafts reported to range between 1880 N and 2664 N [58;43;45]. In comparison, the compressive strength of the TFE + Brh formulation, which translates to approximately 1146 N, suggests that it could effectively contribute to stabilizing the graft by providing additional support in the bone tunnel. This stabilization is crucial in the early weeks post-surgery when the graft is still vulnerable, and the surrounding bone is integrating with the graft tissue. In addition to its compressive strength, the TFE + Brh sample's slightly improved failure strain indicates that it can accommodate small deformations without immediate failure, which could be advantageous in scenarios where some degree of movement is expected post-implantation. This property aligns with the need for a balance between strength and flexibility in materials used in ligament reconstruction, as overly stiff materials could lead to complications such as graft impingement or premature failure due to lack of adaptability to the dynamic forces in the knee joint [57;43;45].

In conlusion, the tensile and compressive tests performed on the TF, TFE, and TFE + Brh formulations provide insight into the mechanical behavior of the materials under different loads. The addition of electrospun Pcl fibers in the TFE formulation enhanced the tensile properties without sacrificing flexibility, suggesting better performance under stress. Similarly, the TFE + Brh sample showed improved compressive strength, indicating its suitability for stabilizing grafts during early-stage recovery in ACL reconstruction. This balance between strength and flexibility supports the use of these formulations in dynamic environments where both tensile and compressive forces are critical. Furthermore, the TFE + Brh formulation's compressive strength of approximately 1146 N, although lower than the maximum forces endured by an ACL, aligns with the lower forces typically required during the early healing phase.

Thus, these results suggest that the TFE + Brh formulation could contribute to better graft anchoring and fixation during the critical post-surgery recovery period.

Table 6 *- Mechanical Tests results*

		UTS (MPa)	US (%)	Failure Stress (MPa)	Failure Strain (%)	Yield Stress (MPa)
Tension	TF	6,9 ± 1,1	11,7	6,3 ± 1,34	14,9	5,5 ± 0,50
	TFE	7,6 ± 0,6	14,9	7,6 ± 0,63	14,9	6,2 ± 0,70
	TFE + Brh	7,0 ± 0,9	12,7	7,0 ± 0,90	12,7	4,6 ± 0,52
Compression	TF	9,1 ± 2,8	7,8	9,1 ± 2,8	7,8	8,9 ± 1,1
	TFE	9,1 ± 2,4	7,3	9,4 ± 2,9	7,3	9,1 ± 2,1
	TFE + Brh	10,6 ± 0,2	7,7	10,6 ± 0,2	7,7	10,6 ± 0,4

3.4. *In vitro* cell culture – Cytotoxicity assays

3.4.1. Alamar Blue test

The Alamar Blue assay results (Figure 30) for the Tunnel Filler samples TF, TFE, and TFE + Brh over 24, 48, and 72 hours demonstrate consistent trends for all formulations. The fluorescence values show that cell metabolic activity remains relatively stable across the different formulations, and significatively higher compared to the positive control for cytotoxicity (DMSO condition), indicating no cytotoxicity.

Although TFE initially shows slightly higher cell viability at the 24-hour mark, by 48 and 72 hours, TFE + Brh performance aligns closely with TFE, indicating that TFE + Brh effectively supports cell proliferation.

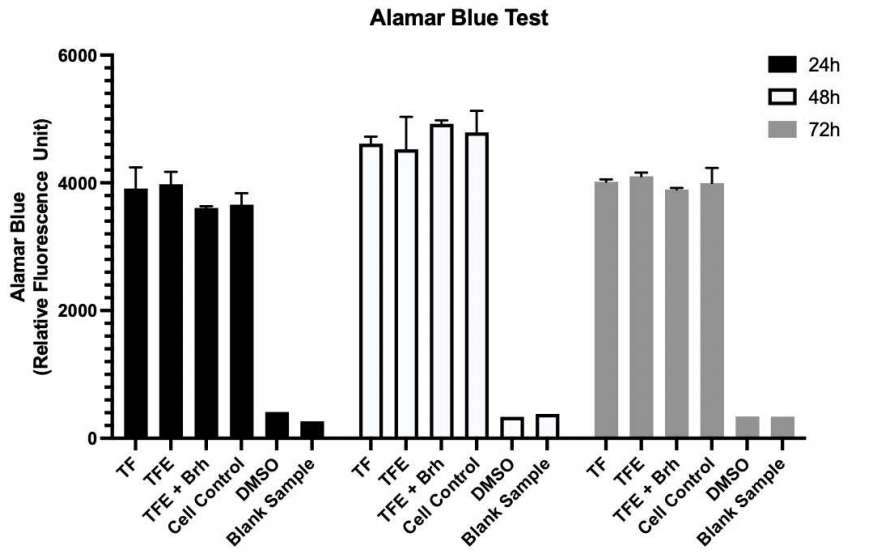

***Figure* 30 -** *Comparison between Alamar Blue test results for each sample in each timepoint tested*

To further validate these findings, a two-way repeated-measures ANOVA was conducted to evaluate the effects of both time and the different formulations on cell viability. The analysis showed a statistically significant effect of time ($P = 0.0026$), although time contributed only 2.099% to the overall variation in the data, indicating that while time had an impact, it was relatively minor. Furthermore, the interaction between time and sample type was not significant ($P = 0.8733$), suggesting that the differences in the formulations' effects on cell viability remained consistent across all time points. Overall, the statistical analysis confirms that the differences in cell viability between the formulations (TF, TFE, and TFE + Brh) are statistically significant, with the formulations TFE and TFE + Brh standing out for their strong performance in promoting cell proliferation over time.

In future, direct contact assays with osteoblasts will be performed to assess if Brh plays a critical role in cell attachment and proliferation. However, we envision that the inclusion of Brushite makes TFE + Brh a particularly promising formulation as TF, where

both immediate biocompatibility and long-term bone regeneration are essential for successful fixation outcomes.

3.4.2. Live/Dead test

The Live/Dead assay conducted over 24, 48, and 72 hours for the Tunnel Filler samples (TF, TFE and TFE + Brh) consistently demonstrated high levels of cell viability (Figure 31). Throughout these time points, green fluorescence (indicative of live cells) was predominant across all samples, with minimal red fluorescence (indicative of dead cells). The control samples functioned as expected, confirming the validity of the experiment, while the DMSO samples, used as positive controls for cytotoxicity, displayed increased cell death, further validating the assay.

- **24h:** All samples exhibited strong green fluorescence with minimal red staining, indicating that the Tunnel Fillers are initially non-cytotoxic
- **48h:** Cell viability remained high across all conditions, with TFE and TFE + Brh showing a slight increase in cell density compared to 24 hours, the same pattern as observed in the negative control for cytotoxicity.
- **72h:** Cell viability continued to be high after 72 hours of culturing, following the same pattern of cell density across all samples, as compared to the negative control for cytotoxicity.

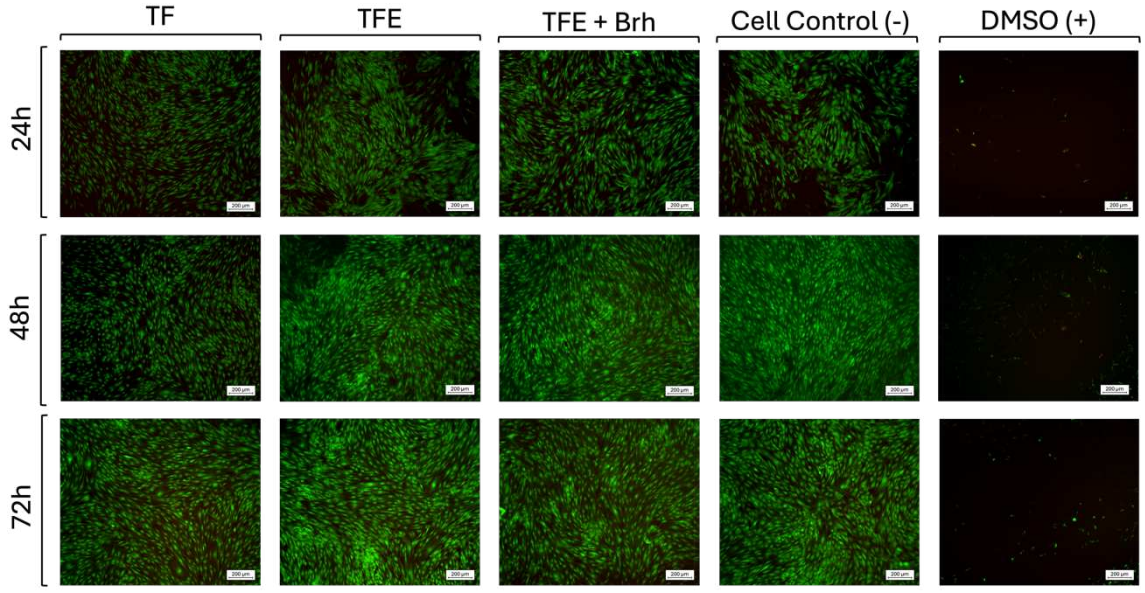

***Figure* 31** - *Live/Dead Test results*

The consistent cell viability observed in all Tunnel Filler formulations (over 72 hours corroborates the previous metabolic activity results and suggests that these materials are cytocompatibility.

In summary, the consistent results across 24, 48, and 72 hours strongly indicate that the TFE + Brh formulation can be suitable for applications such as ACL reconstruction, where high biocompatibility, osteoconductivity, and the ability to support cell proliferation are essential. However, further *in vitro* cell culture tests such as direct contact assays using osteoblasts should be performed to proof the potential of the develop TF. Additionally, further studies, including *in vivo* testing would be valuable in confirming these findings and exploring the full potential of these Tunnel Fillers in orthopedic surgery [59;60].

4. Conclusions

In this thesis, a TF was developed and characterized as a novel approach to address the challenges associated with anchoring and fixation mainly in ligament replacement surgeries. The TF was produced through 3D printing, combined with electrospun fibers, and a brushite coating was applied to improve bioactivity and osteoconductivity.

From a biological perspective, the cytotoxicity assays (Alamar Blue and Live/Dead tests) indicated that the developed TF materials were non-cytotoxic, which is a promising finding for future applications in orthopedics. The incorporation of brushite enhanced the material's bioactivity, providing a scaffold that could promote osteointegration and bone regeneration in future studies. The SEM analysis further reinforced these findings by providing a detailed view of the surface morphology of the samples. The electrospun fibers in the TFE sample introduced surface roughness. FTIR spectroscopy confirmed the chemical integrity of the Pcl structure across all samples, with the successful integration of Brushite in the TFE + Brh sample confirmed through the appearance of phosphate-related peaks. The swelling tests provided additional insight into the functional properties of the materials. The TFE + Brh sample showed the highest swelling capacity, which suggests enhanced liquid absorption due to the presence of the Brushite coating.

Mechanical testing revealed that the developed TF displayed moderate tensile and compressive strength, suggesting a capacity to provide mechanical stability during the early recovery phases after surgery. The results showed that the addition of electrospun Pcl fibers and brushite enhanced the mechanical properties without sacrificing flexibility, making the materials suitable for applications requiring both mechanical support and controlled deformation under stress. Despite showing improved compressive strength, the material's mechanical properties remain lower than that of the native ligament, aligning with the expected role of a Tunnel Filler to support graft fixation rather than withstand full mechanical loading

In future, further investigation should be performed to proof the potential of the developed TF. First, long-term *in vitro* studies are necessary to assess the performance of the scaffold under physiological conditions and relevant environment using osteoblasts.

These tests will provide valuable insights regarding the effect of Brh on cell attachment and proliferation. Moreover, exploring the incorporation of growth factors or other bioactive molecules into the scaffold could further enhance its osteoinductive properties, potentially accelerating the healing process and improving integration with host bone. Then, *in vivo* tests with small animal models should be performed to ensure that the developed TF has suitable degradation and do not induce an exacerbated inflammatory response. Then, knee orthotopic models should be used to assess if the TF can withstand the mechanical loads encountered in the knee over time. Additionally, the scalability of this technology should be examined, ensuring that the manufacturing processes can be adapted for large-scale production without compromising the material's quality or performance. Finally, the potential application of this scaffold design in other orthopaedic procedures, such as spinal fusion or the treatment of large bone defects, represents an exciting avenue for future research.

In conclusion, this thesis has contributed to the field of orthopedics by providing a promising new alternative as tunnel filler for ligament fixation. The advancements made herein lay the groundwork for future innovations in the development of biomaterials for orthopedic applications, underscoring the importance of interdisciplinary approaches in addressing complex clinical challenges.

5. Bibliography

[1] Wroble, R. R., & Brand, R. A. (n.d.). Function of knee ligaments: An historical review of two perspectives. *Iowa Orthopaedic Journal*. Retrieved from https://www.ncbi.nlm.nih.gov/books/NBK561512/

[2] Wang, S. (2022). *Biomechanical analysis of the human knee joint*. Journal of Healthcare Engineering. https://doi.org/10.1155/2022/9365362

[3] Woo, S. L.-Y., Hildebrand, K., Watanabe, N., Fenwick, J. A., Papageorgiou, C., & Wang, J. H.-C. (1999). *Biomechanics of knee ligaments: Injury, healing, and repair*. Journal of Biomechanics, 32(4), 423-429. https://doi.org/10.1016/S0021-9290(98)00185-8

[4] Woo, S. L.-Y., Abramowitch, S. D., Kilger, R., & Liang, R. (2006). *Biomechanics of knee ligaments: Injury, healing, and repair*. Journal of Biomechanics, 39(1), 1-20. https://doi.org/10.1016/j.jbiomech.2004.10.025

[5] American Academy of Orthopaedic Surgeons. (n.d.). *Anterior cruciate ligament (ACL) injuries*. OrthoInfo. https://orthoinfo.aaos.org/en/diseases--conditions/anterior-cruciate-ligament-acl-injuries/

[6] Panorama Orthopedics & Spine Center. (n.d.). ACL injuries by the numbers. Retrieved [insert date you accessed the site], from https://www.panoramaortho.com/news/acl-injuries-by-the-numbers/

[7] Kim, S.-G., Kurosawa, H., Sakuraba, K., Ikeda, H., Takazawa, S., Seto, H., & Ishijima, M. (2005). Analysis of the risk factors regarding anterior cruciate ligament reconstruction using multiple-looped semitendinosus tendon. *The Knee*, 12(5), 366-369. https://doi.org/10.1016/j.knee.2004.10.001

[8] Kamien, E., Szmigielski, W., & Kaźmierczak, J. (2013). Age, graft size, and Tegner activity level as predictors of failure in anterior cruciate ligament reconstruction. *The American Journal of Sports Medicine*, 41(9), 2052-2057. https://doi.org/10.1177/0363546513495307d

[9] Madeti, B. K., & Sharma, A. (2019). *Biomechanics of knee joint—A review*. Journal of Clinical Orthopaedics and Trauma, 10(4), 618-623. https://doi.org/10.1016/j.jcot.2019.07.008

[10] Hosseini, A., Lodhia, P., Van de Velde, S. K., Asnis, P. D., Zarins, B., & Gill, T. J. (2012). *Tunnel position and graft orientation in failed anterior cruciate ligament reconstruction: A clinical and imaging analysis*. International Orthopaedics, 36(4), 845-852. https://doi.org/10.1007/s00264-011-1333-4.

[11] Wang, Y., Lei, G., Zeng, C., Wei, J., He, H., Li, X., Zhu, Z., Wang, H., Wu, Z., Wang, N., Ding, X., & Li, H. (2020). Comparative risk-benefit profiles of individual devices for graft fixation in anterior cruciate ligament reconstruction: A systematic review and network meta-analysis. *Arthroscopy: The Journal of Arthroscopic and Related Surgery*. https://doi.org/10.1016/j.arthro.2020.04.023

[12] Benca, E., Zderic, I., Caspar, J., van Knegsel, K., Hirtler, L., Gueorguiev, B., Widhalm, H., & Varga, P. (2021). On measuring implant fixation stability in ACL reconstruction. *Sensors*, 21(6632). https://doi.org/10.3390/s21196632

[13] CZMEDITECH. (n.d.). *PEEK interference screw*. Retrieved August 22, 2024, from https://www.czmeditech.com/PEEK-Interference-Screw-pd46392450.html

[14] Asif, N., Khan, M. J., Haris, K. P., Waliullah, S., Sharma, A., & Firoz, D. (2021). A prospective randomized study of arthroscopic ACL reconstruction with adjustable- versus fixed-loop device for femoral side fixation. *Knee Surgery & Related Research*, 33(42). https://doi.org/10.1186/s43019-021-00124-0

[15] ResearchGate. (n.d.). *Cortical suspensory fixation devices: In the FL group a fixed-loop suture plate* [Image]. Retrieved August 22, 2024, from https://www.researchgate.net/figure/Cortical-Suspensory-Fixation-Devices-In-the-FL-group-a-fixed-loop-Suture-Plate_fig1_360057828

[16] Lee, Y. S., Ahn, J. H., Lim, H. C., et al. (2009). Structural change of soft tissue anterior cruciate ligament reconstructions with cross-pin fixation between

immediate and postoperative 8 weeks: A study with use of magnetic resonance imaging. *The American Journal of Sports Medicine, 37*(2), 285-290. https://doi.org/10.1177/0363546508324691

[17] Henshaw, R., & Rodeo, S. A. (2004). Noninterference screw bone block fixation devices. *Operative Techniques in Sports Medicine, 12*(3), 195-199. https://doi.org/10.1053/j.otsm.2004.08.003

[18] Arthrex. (n.d.). *ACL reconstruction*. Retrieved August 22, 2024, from https://www.arthrex.com/knee/acl-reconstruction

[19] Ribeiro, V. P., Costa, J. B., Carneiro, S. M., Pina, S., Veloso, A. C. A., Reis, R. L., & Oliveira, J. M. (2022). Bioinspired silk fibroin-based composite grafts as bone tunnel fillers for anterior cruciate ligament reconstruction. *Pharmaceutics, 14*(697). https://doi.org/10.3390/pharmaceutics14040697

[20] Groves, C., Chandramohan, M., Chewa, N., & Subedi, N. (2013). Use of CT in the management of anterior cruciate ligament revision surgery. *Clinical Radiology, 68*(6), e552-e559. https://doi.org/10.1016/j.crad.2013.06.001

[21] Ficek, K., Wieczorek, J., Stodolak-Zych, E., & Kosenyuk, Y. (2012). A revised surgical concept of anterior cruciate ligament replacement in a rabbit model. *Engineering of Biomaterials, 113*, 33-34

[22] Tse, B. K., Vaughn, Z. D., Lindsey, D. P., & Dragoo, J. L. (2012). Evaluation of a one-stage ACL revision technique using bone void filler after cyclic loading. *The Knee, 19*(5), 477-481. https://doi.org/10.1016/j.knee.2011.06.013

[23] Dr. Meyer Orthopaedics. (n.d.). *ACL (anterior cruciate ligamentoplasty)*. Retrieved August 22, 2024, from https://www.dr-meyer-orthopaedics.com/operations/knee/cruciate-ligament-surgery/acl-anterior-cruciate-ligamentoplasty/

[24] Bártolo, P. (2011). *Virtual and Rapid Manufacturing: Advanced Research in Virtual and Rapid Prototyping*. CRC Press.

[25] Gibson, I., Rosen, D. W., & Stucker, B. (2010). *Additive Manufacturing Technologies: Rapid Prototyping to Direct Digital Manufacturing*. Springer.

[26] Ngo, T. D., Kashani, A., Imbalzano, G., Nguyen, K. T. Q., & Hui, D. (2018). Additive manufacturing (3D printing): A review of materials, methods, applications and challenges. *Composites Part B: Engineering, 143*, 172-196.

[27] Woodruff, M. A., & Hutmacher, D. W. (2010). The return of a forgotten polymer—Polycaprolactone in the 21st century. *Progress in Polymer Science*, 35(10), 1217-1256.

[28] Park, J.-S. (2010). Electrospinning and its applications. *Advances in Natural Sciences: Nanoscience and Nanotechnology, 1*(4), 043002. https://doi.org/10.1088/2043-6262/1/4/043002

[29] Martins, A., Reis, R. L., & Neves, N. M. (2008). Electrospinning: Processing technique for tissue engineering scaffolding. *International Materials Reviews, 53*(5), 257-274. https://doi.org/10.1179/174328008X353547

[30] Agarwal, S., Wendorff, J. H., & Greiner, A. (2008). Use of electrospinning technique for biomedical applications. *Polymer, 49*(26), 5603-5621. https://doi.org/10.1016/j.polymer.2008.09.014

[31] Charrière, E., Terrazzoni, S., Pittet, C., Mordasini, P., Dutoit, M., Lemaitre, J., & Zysset, P. (2001). Mechanical characterization of brushite and hydroxyapatite cements. *Biomaterials, 22*(22), 2937-2945. https://doi.org/10.1016/S0142-9612(01)00041-2

[32] Arifuzzaman, S. M., & Rohani, S. (2004). Experimental study of brushite precipitation. *Journal of Crystal Growth, 267*(3-4), 624-634. https://doi.org/10.1016/j.jcrysgro.2004.04.024

[33] Alkhraisat, M. H., Rueda, C., Mariño, F. T., Torres, J., Jerez, L. B., Cabarcos, E. L., & Gbureck, U. (2008). Electroplating of hydroxyapatite-brushite coating on metallic bioimplants with advanced hemocompatibility and

osteocompatibility properties. *Journal of Materials Science: Materials in Medicine, 19*(4), 1807-1815. https://doi.org/10.1007/s10856-007-3264-8

[34] BSc in Bioengineering: Biomedical Engineering, UC: Biomaterials I, 3rd Year 2023-2024. "Production of Hydroxyapatite by a Wet Mechanochemical Method." Protocol Document, University Curriculum, 2023-2024

[35] Borra, R. C., Lotufo, M. A., Gagioti, S. M., Barros, F. M., & Andrade, P. M. (2009). A simple method to measure cell viability in proliferation and cytotoxicity assays. *Braz Oral Res, 23*(3), 255-262. https://doi.org/10.1590/S1806-83242009000300001

[36] Zhou, S., Cui, Z., & Urban, J. (2011). Dead cell counts during serum cultivation are underestimated by the fluorescent live/dead assay. *Biotechnology Journal*, 6(5), 513-518. https://doi.org/10.1002/biot.201000254

[37] Sadeh, N., Oni-Biton, E., & Segal, M. (2016). Acute Live/Dead Assay for the Analysis of Toxic Effects of Drugs on Cultured Neurons. *Bio-protocol*, 6(15), e1889. https://doi.org/10.21769/BioProtoc.1889

[38] Harvey, A., Thomas, N. P., & Amis, A. A. (2005). Fixation of the graft in reconstruction of the anterior cruciate ligament. *Journal of Bone and Joint Surgery - British Volume*, 87-B (5), 593-603. doi:10.1302/0301-620X.87B5.15803

[39] Arliani, G. G., Pereira, V. L., Leão, R. G., Lara, P. S., Ejnisman, B., & Cohen, M. (2019). Treatment of anterior cruciate ligament injuries in professional soccer players by orthopedic surgeons. *Revista Brasileira de Ortopedia*, 54(6), 703-708. doi:10.1055/s-0039-1697017

[40] Mokhena, T. C., & *Other Authors*. (2024). Electrospun PCL-based materials for health-care applications: An overview. *Macromolecular Materials and Engineering*. Wiley Online Library. https://doi.org/10.1002/mame.202400123

[41] Metwally, S., Ferraris, S., Spriano, S., Krysiak, Z. J., Kaniuk, Ł., Marzec, M. M., Kim, S. K., Szewczyk, P. K., Gruszczyński, A., Wytrwal-Sarna, M., Karbowniczek, J. E., Bernasik, A., Kar-Narayan, S., & Stachewicz, U. (2020). Surface potential and roughness controlled cell adhesion and collagen formation in electrospun PCL fibers for bone regeneration. *Materials & Design, 194*, 108915. https://doi.org/10.1016/j.matdes.2020.108915

[42] Musahl, V., Abramowitch, S. D., Gabriel, M. T., Debski, R. E., Hertel, P., Fu, F. H., & Woo, S. L.-Y. (2003). Tensile properties of an anterior cruciate ligament graft after bone–patellar tendon–bone press-fit fixation. *Knee Surgery, Sports Traumatology, Arthroscopy, 11*(1), 68–74. https://doi.org/10.1007/s00167-003-0354-y

[43] Santacroce, L., Charitos, I. A., & Ballini, A. (2023). Ceramic materials for biomedical applications: An overview on properties and fabrication processes. *Journal of Functional Biomaterials, 14*(3), 146. https://doi.org/10.3390/jfb14030146

[44] IntechOpen. (n.d.). Brushite: Synthesis, properties, and biomedical applications. Retrieved from https://www.intechopen.com

[45] Li, X., et al. (2020). Calcium phosphate ceramics: Properties and applications. *ACS Omega, 5*(10), 10948-10957. https://doi.org/10.1021/acsomega.0c00727

[46] Li, W.-J., Laurencin, C. T., Caterson, E. J., Tuan, R. S., & Ko, F. K. (2002). Electrospun nanofibrous structure: A novel scaffold for tissue engineering. *Journal of Biomedical Materials Research, 60*(4), 613-621.

[47] Sill, T. J., & von Recum, H. A. (2008). Electrospinning: Applications in drug delivery and tissue engineering. *Biomaterials, 29*(13), 1989-2006.

[48] Dorozhkin, S. V. (2012). Dissolution mechanism of calcium apatites in acids: A review of literature. *World Journal of Orthopedics, 3*(1), 1-15.

[49] Vasita, R., & Katti, D. S. (2006). Nanofibers and their applications in tissue engineering. *International Journal of Nanomedicine*, 1(1), 15-30.

[50] Tamimi, F., Sheikh, Z., & Barralet, J. (2012). Dicalcium phosphate cements: Brushite and monetite. *Acta Biomaterialia*, 8(2), 474-487.

[51] Li, X., Xie, J., & Lipner, J. (2009). Electrospinning of Nanofibers: Reinventing the Wheel? *Nano Today*, 4(4), 288-298.

[52] Labet, M., & Thielemans, W. (2009). Synthesis of polycaprolactone: a review. *Chemical Society Reviews*, 38(12), 3484-3504.

[53] Leung, V., & Ko, F. (2011). Biomedical applications of nanofibers. *Polymers for Advanced Technologies*, 22(3), 350-365.

[54] Stähli, C., Bohner, M., Miron, R. J., & Dorfer, C. E. (2007). Calcium phosphates in early bone regeneration: a histological study of Brushite and Monetite cements. *Biomedical Materials*, 2(1), 34-39.

[55] Li, X., He, J., Bian, W., Li, Z., Zhang, W., Li, D., & Snedeker, J. G. (2014). A novel silk-based artificial ligament and tricalcium phosphate/polyether ether ketone anchor for anterior cruciate ligament reconstruction – Safety and efficacy in a porcine model. *Acta Biomaterialia, 10*(8), 3696–3704. https://doi.org/10.1016/j.actbio.2014.05.015

[56] Smeets, K., Claes, S., Andrianne, Y., & Verdonk, P. (2021). Current trends in graft choice for anterior cruciate ligament reconstruction – part I: anatomy, biomechanics, graft incorporation and fixation. *Journal of Experimental Orthopaedics*, 8(1), 1-10. https://doi.org/10.1186/s40634-016-0047-z

[57] Woo, S. L.-Y., Debski, R. E., Withrow, J. D., & Janaushek, M. A. (1999). Biomechanics of knee ligaments: injury, healing, and repair. *Journal of Biomechanics*, 32(5), 519-530. https://doi.org/10.1016/S0021-9290(98)00178-X

[58] Harris, J. D., Abrams, G. D., Bach, B. R., Williams, D., & Friel, N. A. (2016). Current trends in graft choice for anterior cruciate ligament reconstruction – part I: anatomy, biomechanics, graft incorporation and fixation. *Journal of*

Experimental Orthopaedics, 3(1), 1-10. https://doi.org/10.1186/s40634-016-0047-z

[59] Stähli, C., Heuberger, R., Klenke, F. M., Meyer, P., & Schlegel, U. (2016). Brushite cement for bone regeneration: a study on its use in cancellous bone defects in sheep. *Journal of Biomedical Materials Research Part A*, 104(4), 965-974.

[60] Ginebra, M. P., Rilliard, A., Fernández, E., Elvira, C., Román, J. S., & Planell, J. A. (2006). Mechanical and rheological improvement of a calcium phosphate cement by the addition of a polymeric drug. *Biomaterials*, 22(13), 1759-1767.